Single-cell transcriptomic analysis of neuro-immune interaction in *Candida albicans*-induced itch mouse model

Alina Tyo

Department of Medical Science

Graduate School

Yonsei University

Single-cell transcriptomic analysis of neuro-immune interaction in *Candida albicans*-induced itch mouse model

Advisor Chang Ook Park

A Master's Thesis Submitted
to the Department of Medical Science
and the Committee on Graduate School
of Yonsei University in Partial Fulfillment of the
Requirements for the Degree of
Master of Medical Science

Alina Tyo

June 2025

Single-cell transcriptomic analysis of neuro-immune interaction in *Candida albicans*-induced itch mouse model

This Certifies that the Master's Thesis of Alina Tyo is Approved

Committee Chair	Je-Wook Yu
Committee Member	Chang Ook Park
Committee Member	Sang Eun Lee

Department of Medical Science
Graduate School
Yonsei University
June 2025

ACKNOWLEDGEMENTS

I would like to express my deepest gratitude to my advisor, Professor Chang Ook Park, for his continuous guidance, constant support, and encouragement throughout this research.

I am also sincerely grateful to the Members of my Thesis Committee, Professor Je-Wook Yu and Professor Sang Eun Lee, for sharing their time to review my work and provide me with their insightful comments and valuable feedback.

I would like to express my great appreciation and gratitude to my lab members Kelun Zhang, Hye Li Kim, Su Min Kim, Yuri Kim, Kyoung do Mun, Yeong Woo Jung, Nicole Bischof, Jiwoo Choi, Wanjin Kim, Jeongmin Cha for their great help and kind support through the whole graduate studies.

Finally, I would like to thank my parents, sister, aunt, grandparents and my friends for their love, kindness, and constant support during my studies abroad. I cannot express how much I appreciate and love you.

Alina Tyo

TABLE OF CONTENTS

LIST OF FIGURES

ABSTRACT

Single-cell transcriptomic analysis of neuro-immune interaction in *Candida albicans*-induced itch mouse model

"Itch-scratch cycle" is a debilitating feature that underlies a range of inflammatory dermatoses. Recently, skin has been recognized as a complex barrier organ capable of synchronizing neuronal and immune cells' activation in response to microbiota. *Candida albicans* is a commensal fungus asymptomatically colonizing human barrier tissues including skin. It has been known that any skin barrier dysfunction leads to increased fungal load and subsequent activation of T_H17 cells. However, the precise mechanisms of pruritis in *C. albicans* skin infection are yet to be discovered. Therefore, in this study we aimed to establish a murine model of *C. albicans* skin infection and assess itch behavioral phenotype. Type 2 immune response is a well-known mechanism in mediating itch sensation. To explore the precise mechanisms of pruritis and involvement of Type 2 immune response in *C. albicans*-induced itch mouse model, we performed single cell RNA sequence analysis of mouse skin and dorsal root ganglion (DRG) cell-cell interaction. Thus, this research aims to be one of the initial studies contributing to exploration of mechanisms underlying *C.albicans*-induced itch sensation via single cell transcriptomic approach.

Key words : *Candida albicans*, pruritis, neuro-immune interaction, dorsal root ganglion, Type 2 immunity

1. Introduction

The term “itch” (pruritis) was first introduced in XVII century to describe an unpleasant sensation that evokes the desire to scratch[1,2]. Being acute, itch plays a protective role for a human body by inducing scratch to get rid of any external factors that may cause harm to it. However, chronic itch due to its pathological origin may become a heavy burden for patients suffering from such inflammatory skin diseases as atopic dermatitis and psoriasis[1,2,3]. It is well known that immune cells are involved in mediation of itch sensation, in particular, T helper 2 (T_H2) cells that mainly release IL-4, IL-13, IL-31 cytokines – crucial mediators of chronic itch in atopic dermatitis which in turn activate their receptors located on the surface of sensory nerves innervating skin[2,3,4]. Thus, the interaction between the immune system and the nervous system has become a basis for the development of neuroimmunology, an interdisciplinary field that focuses on studying integration between immunologic pathways and itch-specific circuits in the nervous system[1-4].

Peripheral sensation such as itch, pain, temperature, and touch are transmitted via the cutaneous sensory nerves toward the dorsal root ganglion (DRG) located near the spinal cord. The DRG is a bundle of sensory neuron bodies that possess long sensory nerve fibers extending to the skin, and are thought to play a critical role in the perception of sensation and the regulation of skin immunity[1,2,3].

Recently, the research interest has shifted toward the interaction between the immune system and the peripheral nervous system (neuro-immune interaction).[1,2,3] In particular, a range of studies is being conducted on neuro-immune interactions in such inflammatory skin diseases as atopic dermatitis[2,4,5] and psoriasis[2,6,7] that manifest by chronic itch and pain sensation. However, the scope of research has been expanding by involving another important component to this interaction – infectious agents that play a crucial role in the development of diseases in a human body[8-12]. Despite the complex and multidisciplinary nature of research related to the immune system, the nervous system and pathogens, its importance makes scientists all over the world change the trajectory of their studies to this direction.

According to studies on inflammatory dermatoses such as atopic dermatitis, psoriasis, and cutaneous T-cell lymphoma manifested by chronic itch, various cytokine receptors are expressed on the terminals of peripheral sensory nerves, whose activation promotes signaling cascades similar to these of immune cells in chronic itch and pain conditions[13,14,15].

However, there are still no reports on sub-molecular mechanisms that can explain accurate mechanisms of itch sensation in each disease.

Candida albicans is an opportunistic fungus that asymptomatically colonizes many areas of the human body including skin. Any alterations in the host immune system leads to the rapid growth of *C.albicans* causing the development of infection[16]. According to the research results of Daniel Kaplan et al., *C.albicans* can directly interact with nerve cells inducing the release of CGRP that in turn triggers the production of IL-23 cytokine by $CD301b^{+}$ dendritic cells (DC), amplifying the IL-17-related immune response. However, the main focus of this study is the regulation of the nervous system's immune response but not the changes in the peripheral nervous system caused by *C.albicans*-induced immune response[12].

Therefore, in this study I plan to explore the transcriptomic and phenotypic changes in sensory nerve cell bodies caused by the immune response to Candida infection that occur in the skin to understand the mechanisms of chronic itch and neuro-immune interaction.

2. MATERIALS AND METHODS

2.1. Application of *C.albicans* to the mouse back skin and oral cavity

Specific pathogen-free, C57BL/6J female mice (6-8-week-old) were purchased from Jackson Laboratory (CA, USA). Mice (n=5/group) were housed in a controlled environment at room T (24 ± 2°C), humidity (55 ± 15%) and a 12-12-h light–dark cycle. Mice were acclimatized for 2 weeks prior to the conduction of the experiment. The hair removal on the mouse upper back part was performed under isoflurane 2% anesthesia using an electric shaver and depilatory protocol. Prior to *C.albicans* application, a Tegaderm film was used for tape-stripping of the shaved mouse back skin (5-7 times) to disrupt the skin barrier[17]. As for the next step, 50 μL from 10^5 CFU/mL of *C.albicans* SC5314 strain was applied to the mouse back skin which was further covered with a Tegaderm film. *Candida albicans* was cultured everyday according to the *C.albicans* culture protocol[18]. A Tegaderm film was removed the following day prior to the behavioral experiment. These procedures were repeated every day with the behavioral checkpoints on day 0, 3, 5, 7, 10 unless otherwise specified. For oral cavity application, we performed mice anesthesia intraperitoneally with ketamine and xylazine (10 μg/g) with additional injection of 1/2 doses if required. A cotton swab saturated with *C.albicans* 10^3 to 10^{10} in 50 μL was subsequently placed to the oral cavity sublingually for 75 min on a daily basis[19]. All experiments were performed following the protocols approved by the Animal Research Ethics Board of Yonsei University (Seoul, Korea).

2.2. Mouse behavioral experiment

To assess itch behavior in mice an infrared Behavior Observation Box (iBOB) equipped with an infrared camera and infrared light source was set up8. Before conducting behavioral experiment, we placed mice for acclimatization to the iBOB for 20-30 minutes. The back model, which is considered to be the standard model for itch assessment in the mouse by allowing to measure scratching in response to itch-evoking stimuli applied to the mouse back was used[20]. A bout of scratch in this experiment was defined as a series of scratches by hind paw toward the Candida albicans-treated mouse back ending with hind paw placed back to the floor. The bouts of scratch were counted for 30 minutes. To confirm the optimal

concentration of *C.albicans* for application to the mouse back with subsequent itch behavior assessment, the oral model of candidiasis was used to differentiate between itch and pain behavior, where a wipe of face by forelimb was equivalent to pain sensation[20]. All videos were assessed blindly by several observers.

2.3. DRG isolation from mouse spinal cord

DRG dissection and isolation was performed and modified according to the previously reported Protocol.[21] On the day of DRG isolation mice were sacrificed using CO_2 gas chamber according to the protocol approved by the Animal Research Ethics Board of Yonsei University (Seoul, Korea). DRGs were collected from healthy and Candida albicans infected mice (n=6/group) from the cervical, thoracic and lumbar segments of spinal cord. After being isolated, DRGs were placed into NBM (500 mL NBM (Invitrogen 21103-049), B27 serum-free supplement (10 mL) (50x, Invitrogen 17504-044), L-Glutamine (5 mL) (Invitrogen 25030-164), 5 mL Pen/Strep (Cellgro 15140-163) with subsequent NBM removal and DRG digestion in 2 mL of pre-warmed Collagenase/Dispase solution (C/D) (Dispase II (Roche 04942078001), HEPES-buffered saline (Sigma 51558-50ML), Collagenase A (Roche 10103578001)) for 20 min at 37 °C (repeated twice). As for the next step, DMEM and 10% FBS (RT) were added to the DRGs in 2 mL C/D solution with further resuspension of the cells in 1 mL of DMEM + 10% FBS (RT). The acquired cells were triturated with 18, 21 and 26 gauge needles and a 1 mL syringe with further removal of undissociated material. The cell suspension was gently layered on top of the BSA with further centrifugation at 1100 rpm for 10 min. Resuspended in 20 mL NBM + P/S pellet passed through a 70 μm strainer and was centrifuged for 5 min at 1000 rpm. The cells were further resuspended in NBM and seeded. Passing quality control: 75-90% of cells were viable (Trypan Blue negative) and no cell debris was visible.

2.4. Skin digestion for single cell and flow cytometry

On the day of flow cytometry analysis, mice were sacrificed using CO2 gas chamber according to the protocol approved by the Animal Research Ethics Board of Yonsei University (Seoul, Korea). Fresh skin samples dissected from mouse back were chopped into smaller pieces with further incubation in Collagenase A (1 mg/mL) + 40 μg/mL DNase (Roche, Mannheim, Germany) and 5mM Ca^{++} (Sigma, St. Louis, MO, USA) in a Hanks' Balanced Salt Solution (HBSS) medium with 5% (v/v) FBS 1%, 1M HEPES, 1% L-

glutamine, 1% P/C (penicillin/streptomycin), and 1000X beta-mercaptoethanol (Gibco) incubated with shaking at 37°C during 30 minutes. After been incubated, in order to suspension containing only single cells, we used a 70 μm cell strainer. The obtained single cell suspension of skin samples was incubated with phorbol 12-myristate 13-acetate (PMA, Sigma, 50 ng/mL), ionomycin (Sigma, 1 μg/mL), and golgistop (BD, 2ul/mL) for 6 hours for further flow cytometry analysis.

2.5. Single-cell RNA sequencing of mouse DRG and skin

To conduct single cell RNA sequence analysis, isolated DRG and skin cells from healthy and Candida albicans infected mice were used (n=6/group). Preparation of Sequencing libraries was performed based on the Drop-seq methodology. Around 20,000 cells per each sample were well mixed with the reagents inducing retrotranscription and subsequently transferred into a Chip A Single Cell, which contained the Single Cell 3' Gel Bead suspension and Partitioning Oil which was further placed into a Chromium Single Cell Controller so that cells will be captured within nanoscale droplets that contain reverse transcription reagents and a gel bead. The formed gel bead-in-emulsions (GEMs) were placed to a thermocycler for retro-transcription (the procedure was performed according to the protocol of manufacturer). A single gel bead contained a specific 10X Genomics barcode, an Illumina R1 sequence, a Unique Molecular Identifier (UMI) and a poly-dT primer sequence. Thus, full-length cDNA was produced based on poly-adenylated mRNA in RT reaction with a unique barcode per cell and transcript, by what all cDNA can be tracked back from each single cell. As for the next step, cDNA was processed by fragmentation, end repair and A-tailing double-sided size selection using AMPure XP beads. As for the last step, Illumina adaptors and a sample index were added through PCR using a total number of cycles adjusted to the cDNA concentration. The samples were indexed, and libraries were again subjected to double-sided size selection. For quantification of the libraries the Qubit dsDNA HS Assay Kit (Life Technologies) was used. D1000 ScreenTapes (Agilent Technologies) was used for assessment of cDNA integrity. Paired-end (26+74bp) sequencing (100 cycles) was carried out using HiSeq 4000 device (Illumina).

2.6. Intravital multiphoton microscopy for assessment of mouse ear alterations

We performed anesthesia using ketamine and xylazine (10 μg/g) and 1/2 doses were additionally injected if needed. Mouse ears were subsequently depilated. In order to provide heat support, mice were placed on a heating plate (CU301, Live Cell Instrument, Seoul, Korea) for further ear imaging[22]. An FVMPE-RS (Evident; Olympus, Tokyo, Japan) was used for capturing images. Recording of images was performed at a magnification of 20X/1.0PA with a water immersion objective. The fluorescence was excited using a Mai Tai high-density DeepSee tunable laser (Spectra Physics, Santa Clara, Calif) at 690-1040 nm excitation wavelength. To stimulate red fluorescent protein (RFP), the Mai Tai laser was used at 1040 nm. The processing of the raw imaging data was performed with ImageJ (National Institutes of Health, Bethesda, Md). To assess cell migration, automatic cell tracking was used, which was further supplemented by manual adjustments. To generate graphs from the data, a Prism 8 application package was used (GraphPad Software, La Jolla, Calif). Movies were generated using ImageJ software sequences exported from cellSens (Evident).

2.7. Measurement of *C.albicans*-specific IgE in sera by enzyme-linked immunosorbent assay (ELISA)

Concentration of *C.albicans*-specific IgE were measured using Mouse Anti Candida albicans IgE Antibody ELISA kit (MyBioSource, San Diego, CA, USA). Serum samples were processed according to the manufacturer protocol. Briefly, 100 μL of each Standard (0, 10, 25, 50, 100, 250 ng/mL) and Samples were added to the coated wells with 100 μL of PBS being used as a control in the blank well. Then 50 μL of Conjugate was added to each well excluding the blank control well. After mixing well, the plate was covered and incubated for 1 hour at 370C. After washing five times with Washing Solution and completely removing the liquid, 50 μL of substrate A and 50 μL of substrate B were added to each well with subsequent covering and incubation for 15-20 min at 37^0C. Lastly, 50 μL of Stop Solution was added to each well and mixed. The optical density was determined at 450nm using a microplate reader (TECAN, Salzburg, Austria) instantly.

2.8. Optical Imaging with Voltage-Sensitive Dye (VSDi) for Tracking Neuronal Activity in DRGs

VSDi experiment was conducted according to the previously published protocol[23]. Briefly, on day 10 of *C.albicans* epicutaneous treatment, mice were anesthetized

intraperitoneally with urethane (50 mg/kg). The isolation of DRGs was performed in an optical chamber filled with artificial cerebrospinal fluid (aCSF) equilibrated with a gas mixture (5% CO2in O2; pH 7.4). We performed optical imaging after quick isolation of DRGs in the recording chamber. Staining step was conducted during 1 hour with preparations being placed to aCSF with a voltage-sensitive dye (VSD) (Di-2-ANEPEQ, 50 mg/mL in 0,9% NaCl, Molecular Probes, Eugene, OR, USA). After 1 hour we used fresh aCSF in order to replace staining dye with subsequent performance of optical imaging with a MiCAM02 hardware and data analysis with software package (BrainVision, Tokyo, Japan). MiCAM02 camera and a fixed-stage upright fluorescence microscope (BX51WI, Olympus, Tokyo, Japan) were used for optical imaging. A halogen lamp and a dichroic mirror were used to record the activation of DRGs. Stimulation of DRGs was performed with a concentric bipolar electrode with intensities of 1 and 3 mA.

2.9. Statistical analysis

GraphPad Prism 10.1.2 (GraphPad Software, Inc., San Diego, CA, USA) was used to perform statistical analysis. A Mann-Whitney test was used to determine the difference between the two groups. P-value of < 0.05 was defined as a statistical significance criteria. The downstream analysis of single cell RNA sequence DRG and skin data was conducted using Seurat package 5.1.0 in R 4.4.2. To filter out low quality cells, individual cells with number of genes fewer than 500, nUMI (unique molecule identifiers) fewer than 1000, log10GenesPerUMI lower than 0.8 and mitochondrial genes greater than 10% were removed from the dataset. As for the DRG datasets, non-neuronal cells were also excluded from the analysis. Neuronal and skin immune cell subtypes were clustered using PCA and UMAP analysis referring to the previously published studies on identification of marker genes for distinct DRG neuron and skin immune cell clusters. DEG (differential gene expression) - analysis was conducted using the FindMarker function in Seurat package.

3. RESULTS

3.1. Establishment of *C.albicans*-induced itch mouse model

To assess how *C.albicans* induces itch, we employed and modified cutaneous *C.albicans* infection and S.aureus infection and behavioral murine models. First, we aimed to determine the optimal concentration of *C.albicans* for epicutaneous application that can trigger the most prominent itch behavior. For this, 50 μL of various concentrations of *C.albicans* ranging from 10^3 to 10^{10} CFU/ml were applied to the mouse back on daily basis with subsequent 24 hours-post exposure assessment of itch behavioral phenotype via video recording on day 0, 3 and 5. As shown in Figure 1A, the highest scratching pattern was observed on day 5 when 50 μL of 10^5 CFU/ml was applied. Next, we attempted to define the time point of the highest and most stable itching behavior under *C.albicans* epicutaneous application. Mice were treated with 50 μL of 10^5 CFU/ml for 12 consecutive days with 24 hours post-exposure itch behavioral analysis performed in dynamics on day 0, 3, 5, 7, 10, 12. As a result, compared to control group, *C.albicans*-treated mice showed significantly increased scratching behavior started from day 3 with the most stable pattern being observed on day 10 (Figure 1B and 1C). Taken together the behavioral results, application of 50 μL of *C.albicans* 10^5 CFU/ml daily for 10 consecutive days was confirmed as an established *C.albicans*-induced itch mouse model (Figure 1C). Characteristic *C.albicans*-induced skin inflammatory changes with histologically confirmed epidermal hyperplasia and inflammatory cell infiltrate in dermal layer are shown in Figure 1D.

A

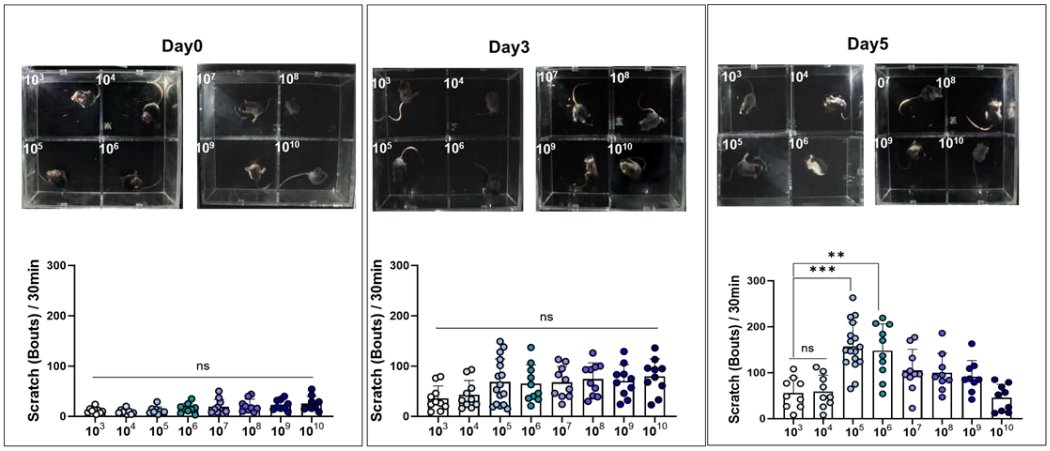

B

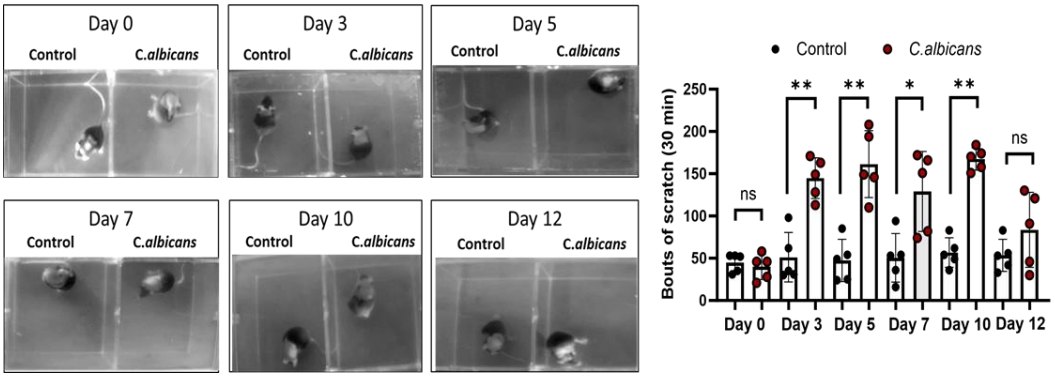

C

Established *C.albicans*-induced Itch Mouse Model

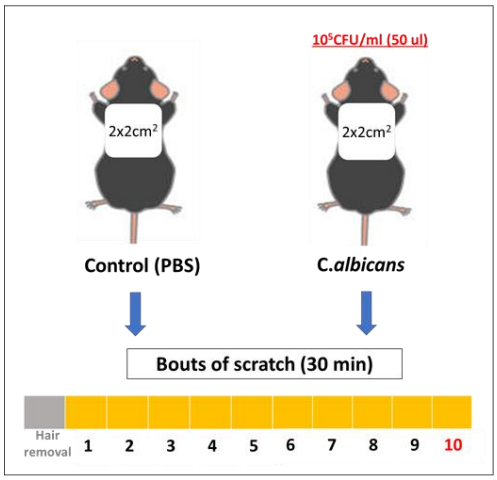

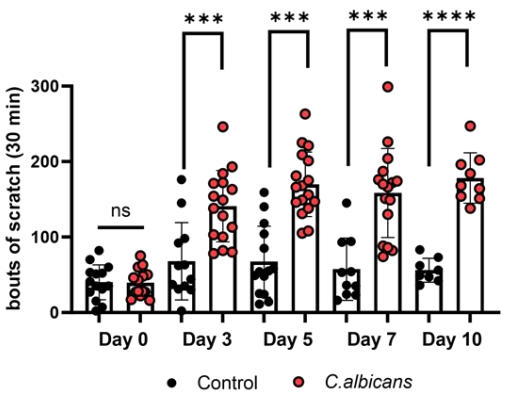

D

Skin alterations in *C.albicans*-induced Itch Mouse Model

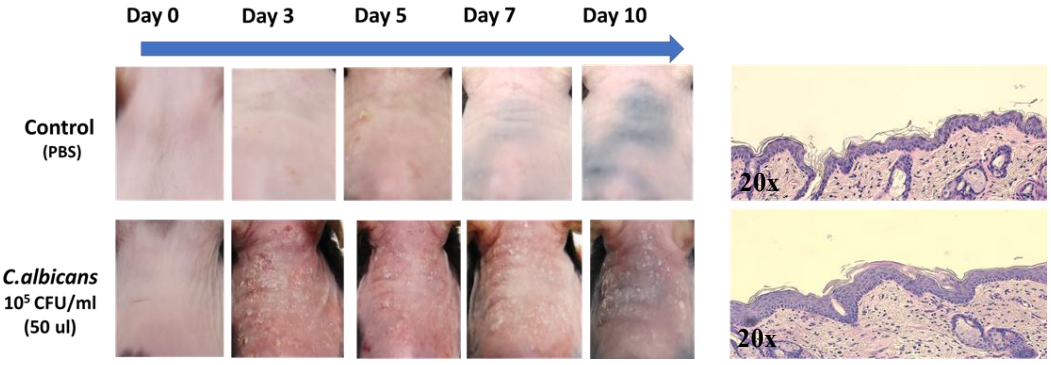

Figure 1. Establishment of *C.albicans*-induced itch mouse model. (A) Scratching behavior of WT mice treated by various concentrations of *C.albicans* starting from low 10^3 to high 10^{10} CFU/ml (50 μL), n ≥ 8 mice per group. (B) Scratching behavior of *C.albicans*-treated WT mice compared to control littermates examined in dynamics on day 0,3,5,7,10 and 12, n = 5 mice per group. (C) Schematic presentation of established *C.albicans*-induced itch mouse model with scratching behavior pattern on day 0,3,5,7 and 10, n ≥ 8 mice / group. (D) Representative time-lapse images of *C.albicans*-induced skin lesions compared to control mouse skin and H&E stained photomicrograph of skin sections from *C.albicans*-treated and control mice. Original magnification x20. Nonparametric Mann-Whitney U tests was performed to analyze statistical significance for (A) -(C). *p<0.05; **p< 0.01; ***p <0.001; ****p < 0.0001; ns, not significant.

3.2. Morphological and electrophysiological changes of sensory neurons in *C.albicans*-induced itch mouse model

3.2.1. Skin Nerve Fiber Remodeling in *C.albicans*-induced itch mouse model

To evaluate structural remodeling of sensory nerve fibers in skin affected by *C.albicans*, Nav1.8-Cre-tdT mouse back and ears were treated with 50 μL of *C.albicans* 10^5 CFU/ml daily for 10 consecutive days according to our established *C.albicans*-induced itch murine model (Figure 2A). On day 10, we performed two-photon microscopy of mouse ears and examined morphological changes of nerve fibers. Our data shows that exposure to *C.albicans* leads to increase of nerve fiber thickness with more than 2-fold changes in comparison with control group (Figure 2B-C). Moreover, we observed significant increase in nerve fiber density following *C.albicans* exposure compared with control mice (Figure 2D).

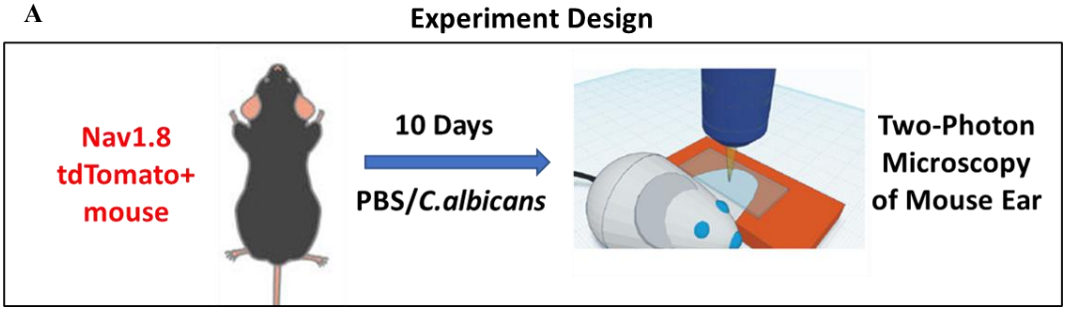

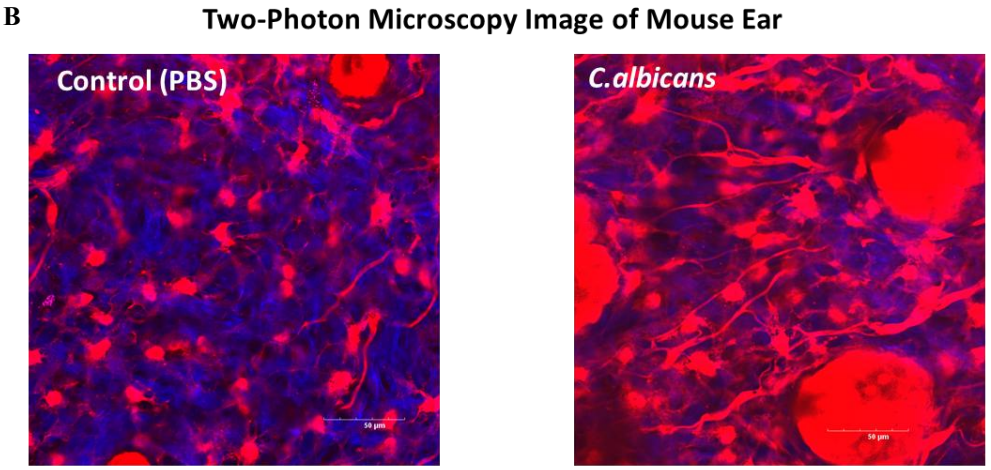

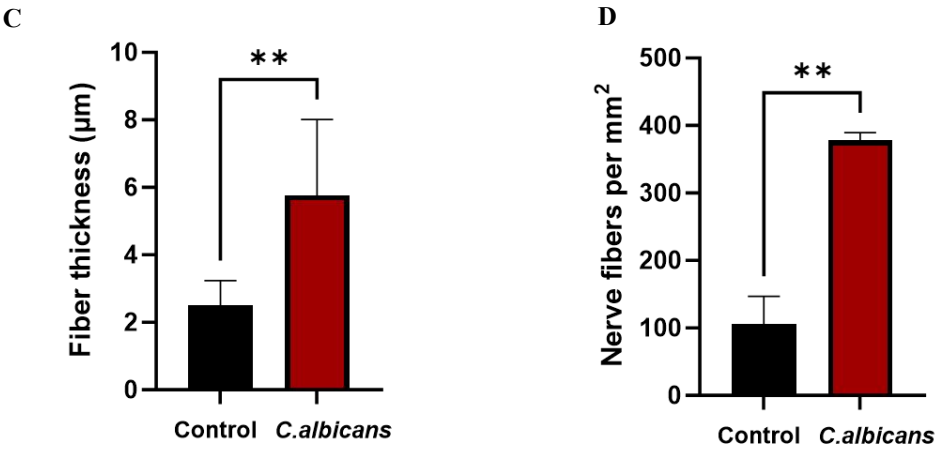

Figure 2. Skin Nerve Fiber Remodeling in *C.albicans*-induced itch mouse model. (A) Experiment design for conducting two-photon microscopy. (B) Two-photon microscopy image of control and *C.albicans*-treated Nav1.8-Cre-tdT mouse ears with subsequent analysis of (C) nerve fiber thickness and (D) nerve fiber density. Each symbol represents nerve fiber per area. Nonparametric Mann-Whitney U tests was performed to analyze statistical significance for (C) and (D). **p <0.01. Scale bars, 50 μm.

3.2.2. Electrophysiological changes of sensory neurons in *C.albicans*-induced itch mouse model

Additionally, we performed VSD imaging to assess neuronal activity of DRGs isolated from WT control and *C.albicans*-treated mice on day 10 (Figure 3A). For this, we recorded changes of DRG's membrane potential in response to electrical stimulation and subsequently tracked DRG neuronal activity (Figure 3B). When stimulated by 1mA, both control and experimental DRGs showed similar neuronal activity as their peak amplitude responses were registered within the same range. However, under 3mA stimulation, higher neuronal activity was observed in *C.albicans*-treated group. Furthermore, we analyzed activated pixel changes of 1mA and 3mA stimulation images. As a result, both 1mA and 3mA stimulation in *C.albicans*-treated group showed pronounced increase in neuronal activity compared to the control group. Thus, our data suggests that *C.albicans*-treated group DRG exhibits higher neuronal activity than DRG from control mice with difference increased in correlation with intensity.

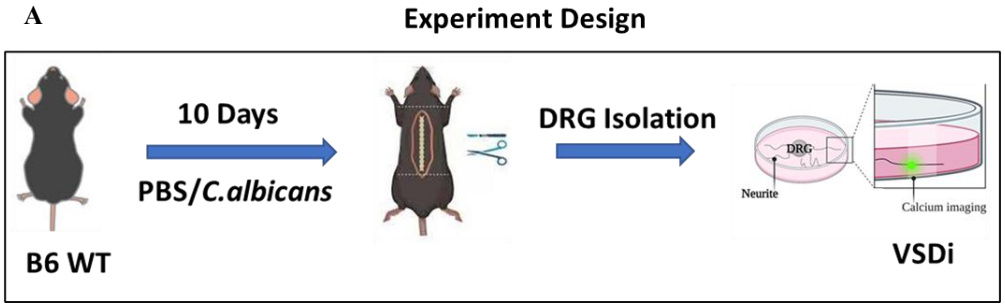

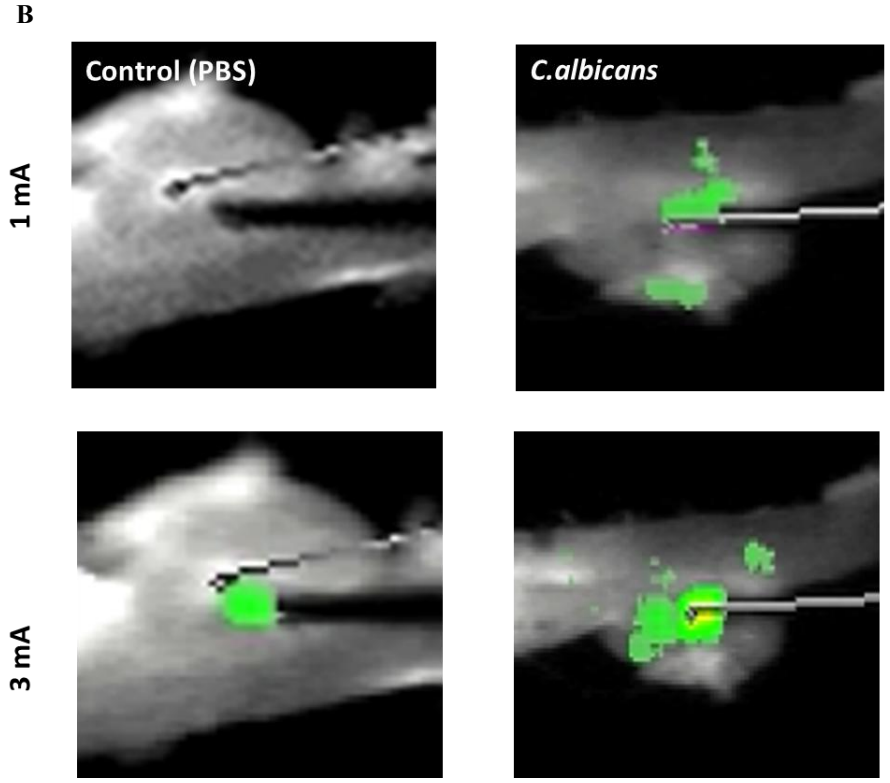

Figure 3. Electrophysiological changes of sensory neurons in *C.albicans*-induced itch mouse model (A) Experiment design for conducting voltage-sensitive dye imaging (VSDi) analysis. (B) Images of optical signals at 1mA and 3mA stimulation of WT control and *C.albicans*-treated mouse DRGs.

3.3. Single cell transcriptomic analysis of DRG and skin in *C.albicans*-induced itch mouse model

3.3.1. Transcriptomic analysis of DRG tissue cells in *C.albicans*-induced itch mouse model

To further explore the precise mechanisms of itch in *C. albicans*-induced itch mouse model, we conducted scRNA sequence analysis of DRG (C1-L2) and skin samples isolated from WT control and *C.albicans*-treated mice (n=6/group), following established protocol (Figure 4A). We obtained the transcriptomic profiles of ~36.940 DRG cells and ~34.737 skin cells from *C.albicans*-treated group and ~35.834 DRG cells and ~42.745 skin cells from their control littermates, which were further clustered and visualized by principal component analysis – PCA, and uniform manifold approximation and projection - UMAP analysis. For analysis of DRG datasets, we began with identification of neuronal and non-neuronal markers of DRG cells to filter out cell types other than neurons including immune cells (*Ptprc, Cd74*)[24], vascular smooth muscle cells (VSMCs) (*Tagln, Myh11*)[25,26], endothelial cells (tight junctions) (*Pecam1, Cldn5*)[24,27], satellite glial cells (SGC) (*Fabp7, Cdh19*)[24,28], fibroblasts (*Col1a2, Dcn, Apod, Mgp*)[24] and Schwann cells (*Mpz, Ncmap, Prx*)[29]. We used specific neuron-related markers such as *Pou4f1*[30], *Avil*[31], *Rbfox1-3*[32,33,34] to identify neuron cells for further clustering (Figure 4B, C, D).

A

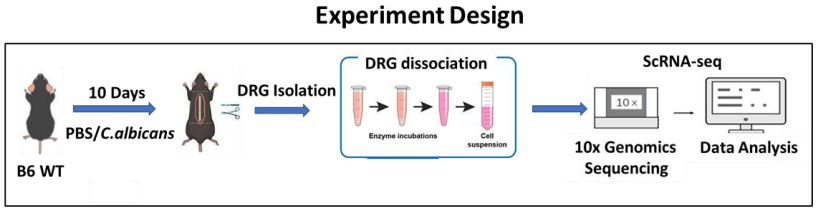

B

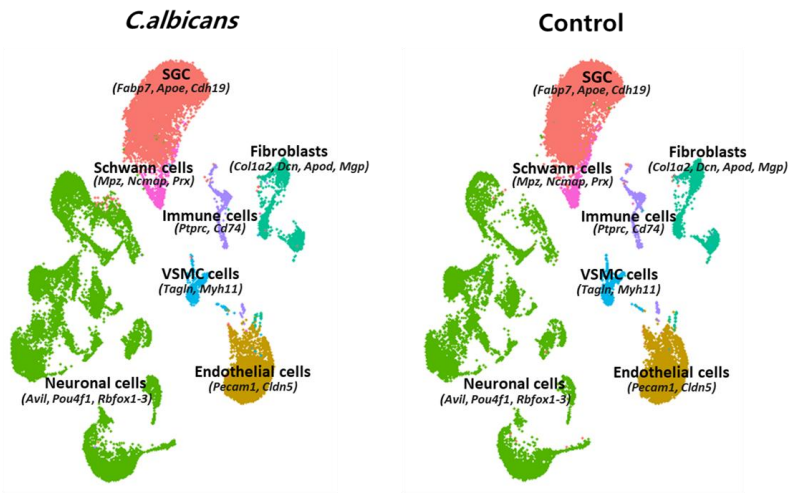

C

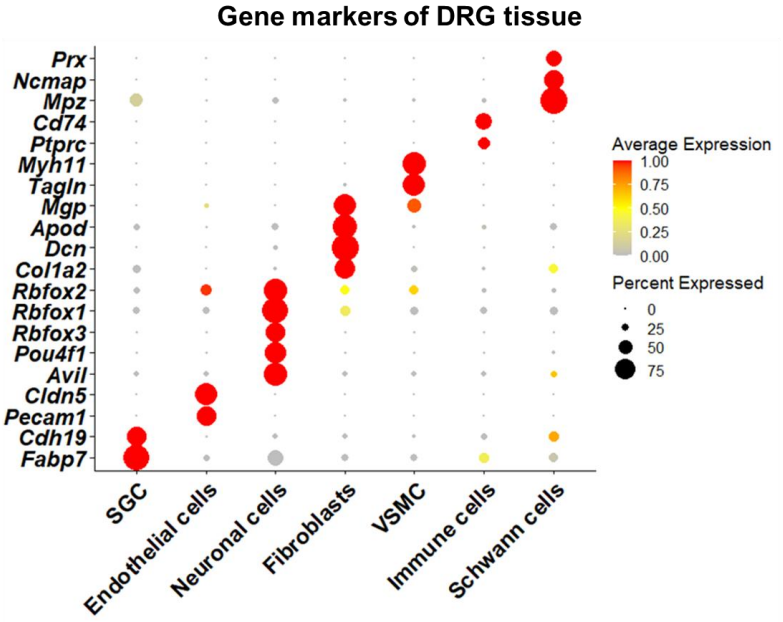

D

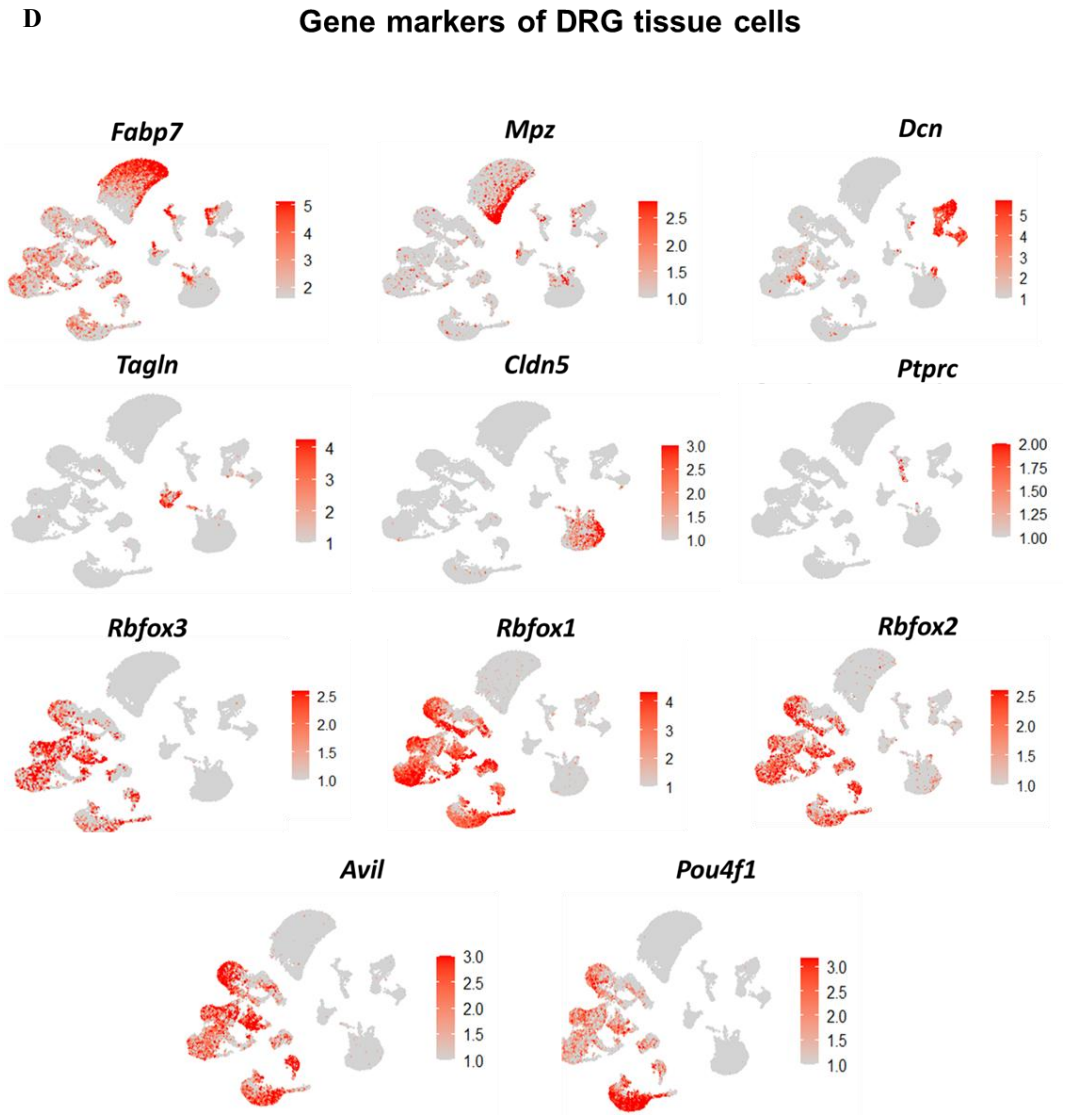

Figure 4. Identification of non-neuronal and neuronal subclusters in mouse DRG tissue. (A) Experiment design for conducting scRNA sequence analysis of DRG. DRGs were dissected and dissociated into single cell suspension with further processing by 10x Genomics. (B) UMAP visualization of mouse DRG tissue showing non-neuronal and neuronal subclusters for further DRG neuronal cells analysis. Dots represents individual cells, colors represent DRG tissue cell clusters. (C) DotPlot and (D) UMAP plot of representative gene markers for distinguishing between non-neuronal and neuronal cell types. The dot size shows the percentage of cells expressing genes corresponding to individual cluster in (C) and individual cells in (D); the color shows the average expression of normalized transcript counts in DRG tissue cells.

3.3.2. Transcriptomic analysis of DRG neuronal cells in *C.albicans*-induced itch mouse model

After re-analyzing DRG neuronal cells, our dataset revealed 13 transcriptionally distinct neuronal clusters based on previously reported marker genes of sensory neurons (Figure 5A). In consistence with published studies[31,35,36] we identified distinct subsets of low threshold mechanoreceptors - C-LTMR (*Th*), Aβ-LTMR (*Ntrk3, Ntng1*), and Aδ-LTMR (*Ntrk2, Cadps2*) – that are responsible for detection of innocuous touch sensation, proprioceptors (Pvalb), distinct peptidergic subsets – PSPEP1 *(Hcrtr1, Prokr2, Smr2)*, PSPEP2/3 *(Oprk1)*, PSPEP4 *(Sstr2)*, PSPEP5 *(Gabrg3, Dcn)*, PSPEP6/7 *(Trpm8)*, PSPEP8 *(Rxfp1)*, and subtype of neurons traditionally annotated as non-peptidergic (NP) neurons – NP1 (*Mrgprd*), NP2 (*Mrgpra3*) and NP3 (*Sst*) (Figure 5A, B). In particular, NP1, NP2 and NP3 are associated with itch-transducing neurons[4,35,37,38], with NP3 cluster being closely related to inflammatory itch sensation. Therefore, we focused on NP neuronal subtypes in our further analysis.

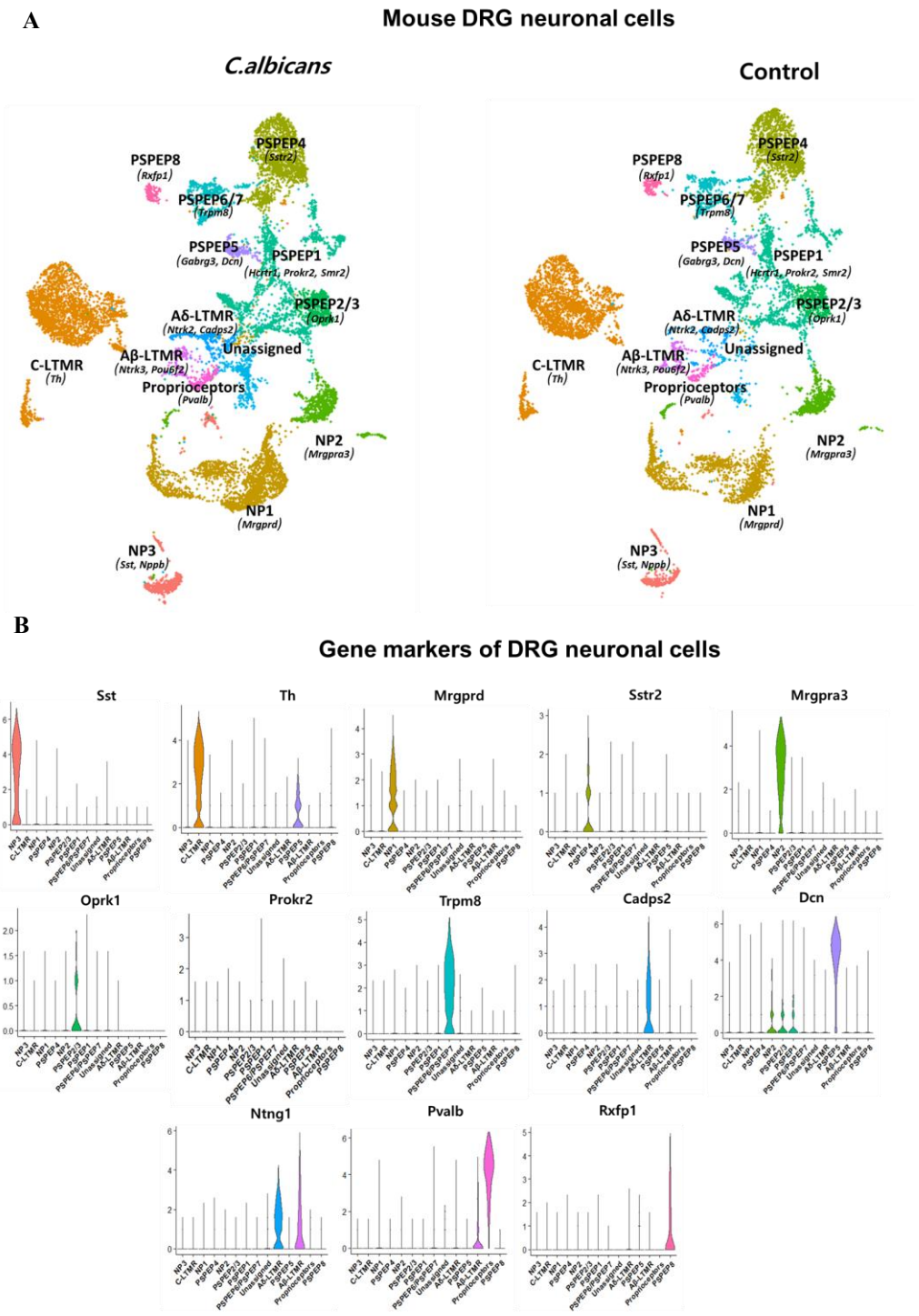

Figure 5. Identification of neuronal cell clusters in mouse DRG tissue. (A) UMAP visualization of 13 distinct DRG neuronal cell subtypes in mouse DRG tissue. Dots represents individual cells, colors represent DRG tissue cell clusters. (B) Violin plot of representative neuronal gene markers' expression for classification of DRG neuronal cells.

3.3.3. Analysis of itch-specific receptors expression in NP clusters

In consistence with previously published studies, NP1 cluster was defined with *Mrgprd*, NP2 – with *Mrgpra3* and NP3 – with *Sst* marker genes[4,35,37,38] (Figure 6A). When analyzing these subsets, we observed enrichment of cells across all NP clusters from *C.albicans* mice DRGs compared to that of the control group. Next, we examined major itch-related receptors in NP clusters. Atopic dermatitis (AD) is a classical inflammatory dermatosis accompanied by severe pruritis and prominent Type 2 immune response[13,39,40]. Therefore, we analyzed expression of Type 2 cytokine receptors – IL-4R (*Il4ra*) and IL-13R (*Il13ra1*). Interestingly, both IL-4R and especially IL-13R along with histamine receptors (histamine H1 receptor (*Hrh1*) and histamine H2 receptor (*Hrh2*)) were upregulated in *C.albicans* group comparing to the control group. Specifically, we observed distinct expression pattern of these receptors depending on NP subset. Thus, IL-13R was upregulated in NP2 cluster, while NP1 neurons were enriched in IL-4R. Moreover, NP2 subset of *C.albicans* group contained more H1 and H2 receptors than that of control mice (Figure 6B). Thus, our results show upregulation of Type 2 immune response-related receptors in sensory neurons highlighting possible involvement of this pathway in mediation of itch signal in response to *C.albicans*.

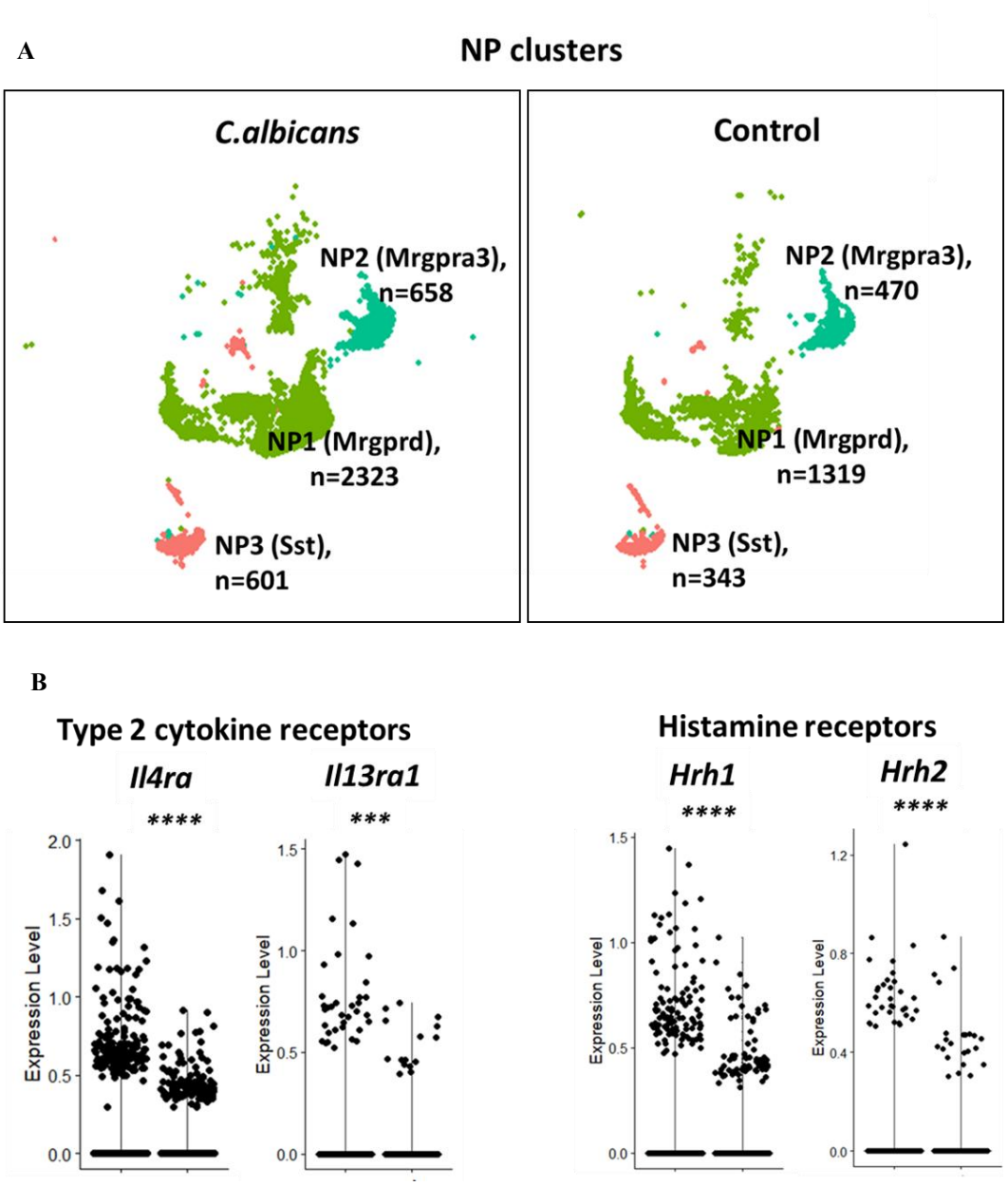

Figure 6. Analysis of itch-specific receptors expression in NP clusters. (A) UMAP visualization of NP1, NP2 and NP3 clusters with further counting of absolute number of cells in each cluster. All NP clusters showed increase in cell number in *C.albicans*-treated group compared to the control mice. Dots represents individual cells; colors represent distinct NP cell clusters. (B) Violin Plot of IL-4R (*Il4ra*) expression in NP1 cluster, IL-13R (*Il13ra1*), H1R (*Hrh1*) and H2R (*Hrh2*) expression in NP2 cluster. Dots represents individual cells. Nonparametric Wilcoxon rank sum test was performed in Seurat to analyze statistical significance for (B). ***p< 0.001; ****p <0.0001.

3.3.4. Transcriptomic analysis of skin tissue cells in *C.albicans*-induced itch mouse model

To further understand the underlying mechanisms of itch induced by *C.albicans*, we conducted analysis on skin samples isolated from WT *C.albicans*-treated mice and their littermates (n=6) (Figure 7A) . Using previously published gene markers, we first identified 7 distinct subsets of cells in skin including fibroblasts (*Col1a2, Dcn, Lum*)[41,42,43], keratinocytes (*Krt1, Krt5, Krt14, Krt15*)[44,45], immune cells (*Ptprc, Cd74*)[24,46], endothelial cells (*Ptprb, Cldn5, Podxl*)[47,48], melanocytes (*Oca2, Sox10, Pax3*)[49,50,51], Schwann cells (*Mpz, Ncmap, Prx*)[29], and adipocytes (*Adig, Cidec*)[48] (Figure 7B, C). In order to focus more on immune cells to explore neuro-immune interaction in our model, we performed re-clustering of $CD45^+$ cells (*Ptprc*).

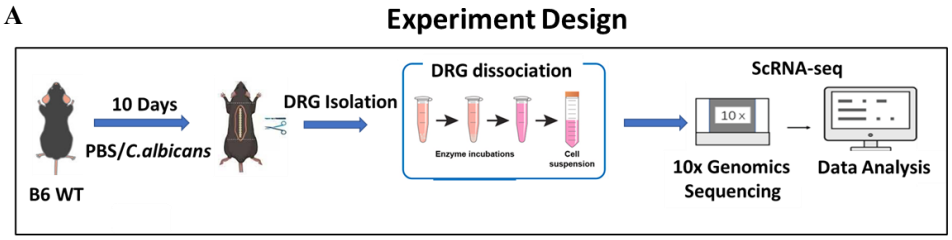

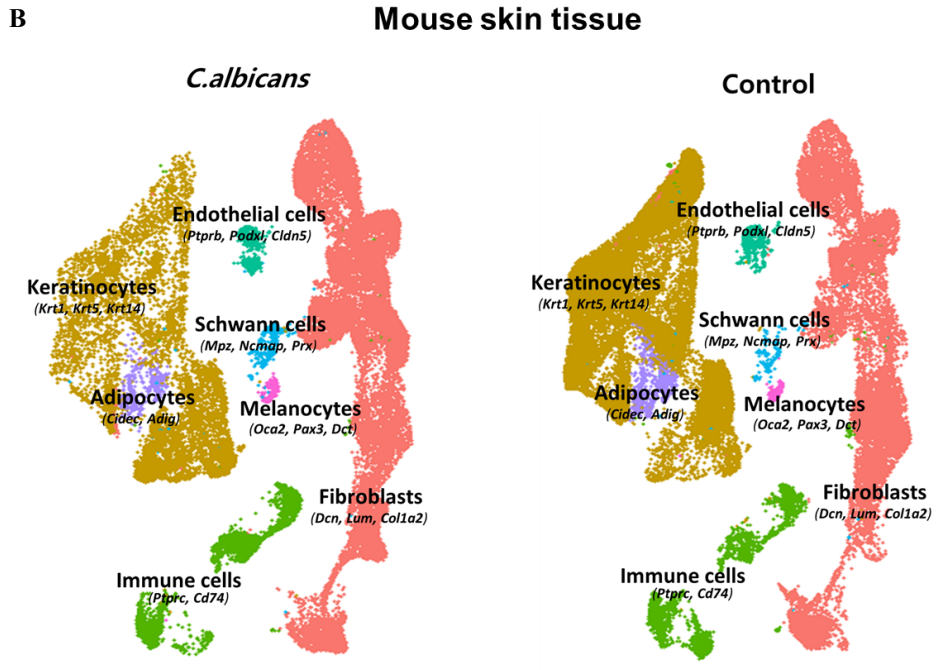

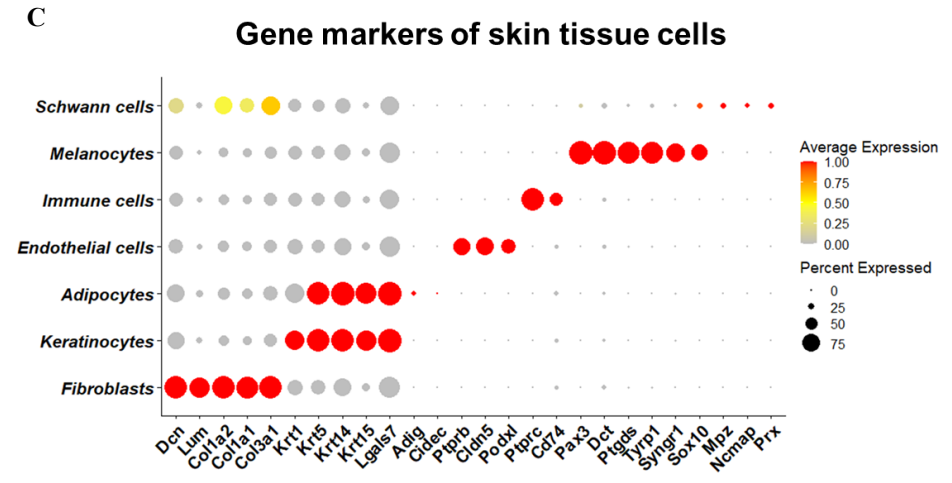

Figure 7. Identification of major cell clusters in mouse skin tissue. (A) Experiment design for conducting scRNA sequence analysis of skin. Skin samples were dissected from *C.albicans* and control groups (n=5/group) with further dissociation into single cell suspension and processing by 10x Genomics. (B) UMAP visualization of major skin cell clusters including fibroblasts, keratinocytes, immune cells ($CD45^+$ cells), endothelial cells, melanocytes and Schwann cells. Dots represents individual cells; colors represent skin tissue cell clusters. (C) Dot Plot of representative gene markers for major skin cell subtypes clustering. The dot size shows the percentage of cells expressing genes corresponding to individual cluster; color shows the average expression of normalized transcript counts in skin tissue cells.

3.3.5. Analysis of skin CD45$^+$ immune cells in *C.albicans*-induced itch mouse model

After sub-clustering CD45$^+$ cells, we identified 11 immune subtypes based on their classical gene markers (Figure 8A). These include macrophages (*F13a1, Adgre1*)[52,53], dendritic cells (*Itgax, Flt3*)[54], Langerhans cells (*Cd207, H2-DMb2*)[55,56], T helper cells - T_H1 (*Tbx21, Ifng*)[57] and T_H2 (*Gata3, Il4, Il5, Il13*)[57], regulatory T cells (Treg) (*Foxp3*))[57], mast cells (*Mcpt4, Tpsb2, Fcer1a*)[58] and neutrophils (*S100a8, S100a9*)[59]. Moreover, we observed non-conventional T cell population - γδ T cells (*Trdc, Trgc1)*[60] that are abundant in peripheral tissues including skin. In particular, resting γδ T cells were found to be in non-activated state as it they did not express cytokine molecules. On the opposite, γδ17 cells (*Trdc, Rorc, Il17a*)[61,62] are actively expressing effector molecules such as IL-17A and IL22 specifically in *C.albicans*-treated group as a classical response to fungal infection. Furthermore, we observed a distinct cluster that did not express canonical CD3 markers, but showed high expression of type 2 immune cells-related genes – *Gata3, Il4, Il13* and *Il5*. Therefore, we identified this subset as ILC2 cells (*Cd3e-, Gata3+*)[63] (Figure 8B, C). According to our dataset analysis, while T_H1, γδ17 and Treg cells can be easily distinguished within the T helper cells cluster, T_H2 master transcription factor *Gata3* expression is highly overlapped with that of *Foxp3*.

A

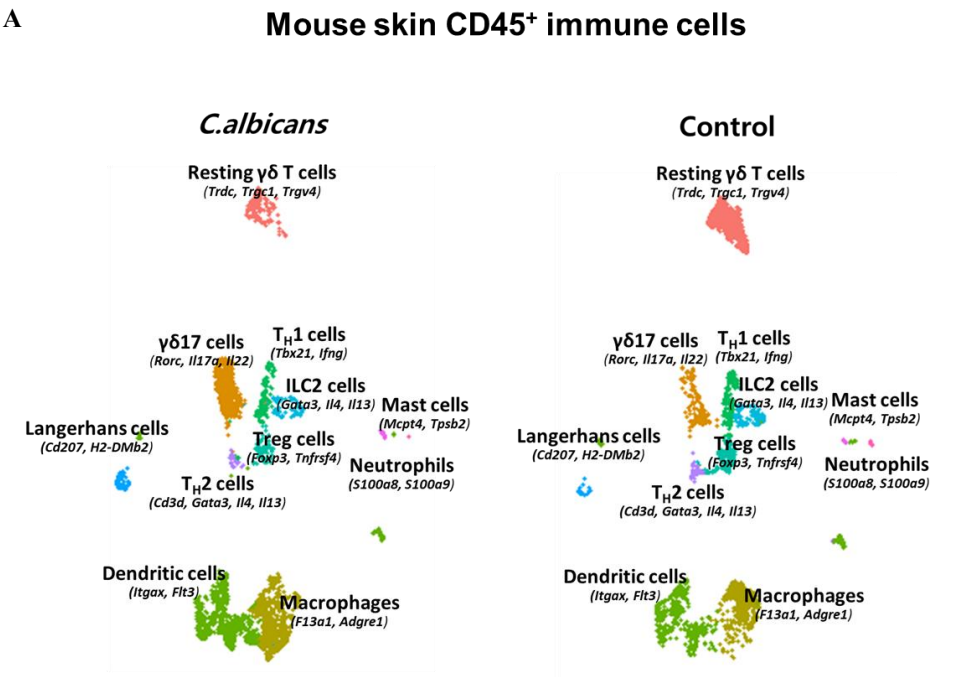

B

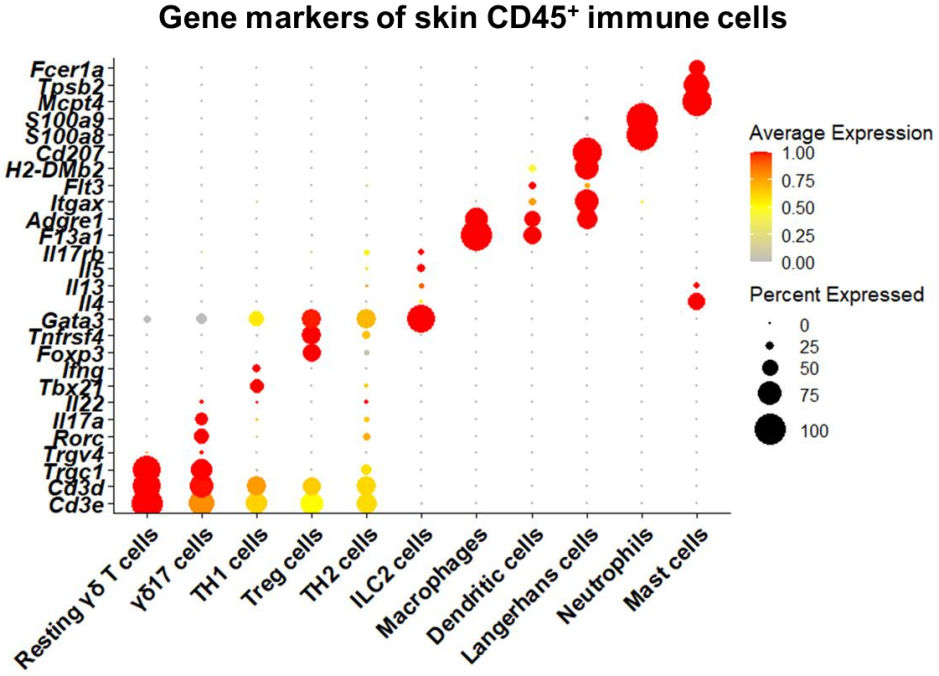

C

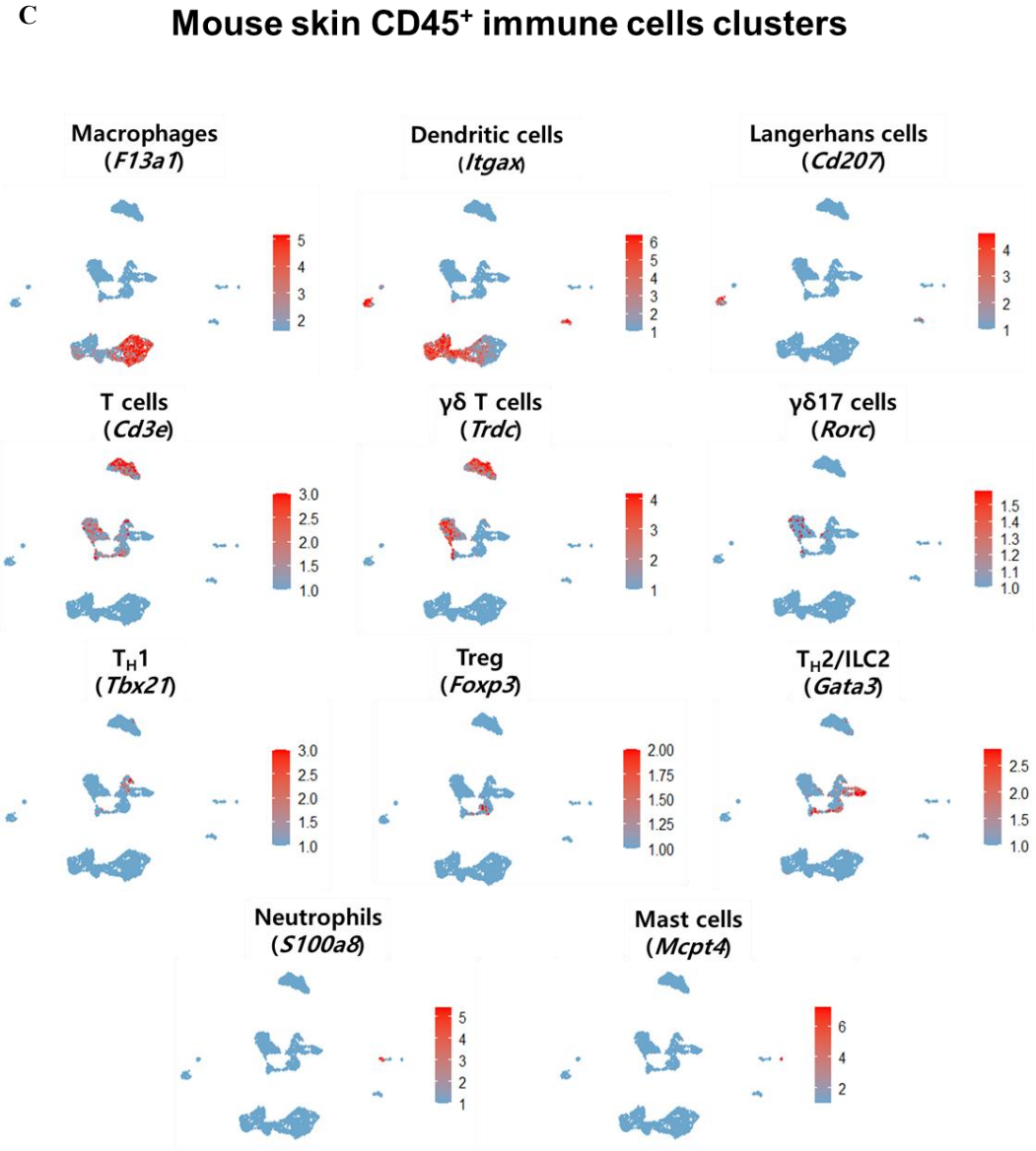

Figure 8. Identification of CD45$^+$ cell clusters in mouse skin tissue. (A) UMAP visualization of 11 distinct CD45$^+$ cell subtypes in mouse skin tissue. Dots represents individual cells, colors represent skin CD45$^+$ immune cells clusters. (B) Dot plot and (C) UMAP plots of representative CD45$^+$ immune cells gene markers' expression for clustering in skin tissue. Dots indicates individual cells in (B) and (C) percentage of skin CD45$^+$ immune cells expressing genes corresponding to individual cluster, and the color represents the average expression of normalized transcript counts in skin CD45$^+$ immune cells.

3.3.6. Assessment of Type 2 immune cells involvement in mediating itch in *C.albicans*-induced itch mouse model

Next, we focused on analysis of T cells and ILC2 subsets. It is widely known that *C.albicans* triggers γδ17 cells activation which, in turn, produce IL-17A and IL-22 cytokines that play crucial role in combating fungal infection and mediating antimicrobial immunity[61,62]. Consistent with this concept, gene expression analysis of our immune cells' dataset revealed pronounced increase in IL-17A and IL22 production in *C.albicans* group compared to the control mice along with upregulation of other type 17-related gene markers (*Rorc, Il17f, Cxcr6*) (Figure 9A). In addition, we examined T_H1 (*Stat4, Il12rb2, Il27ra, Tbx21, Ifng*) (Figure 9B) but did not observe significant difference between two groups. On the contrary, type 2-related gene markers (*Stat6, Il4, Il13, I17rb, Il4ra*) (Figure 9C, D) surprisingly showed tendency to upregulation in type 2 immune cells. Thus, upregulation of Type 2 cytokines (*Il4, Il13*), transcriptional factor *Stat6* and surface markers (*Il17rb)* were observed particularly in ILC2 subset. Moreover, T_H2 cells demonstrated tendency to upregulation of transcriptional factor *Stat6* and surface markers (*Il17rb* and *Il4ra*). Thus, our DRG and skin datasets suggest possible involvement of Type 2 immune response in mediating itch sensation in *C.albicans*-inudced itch mouse model.

A

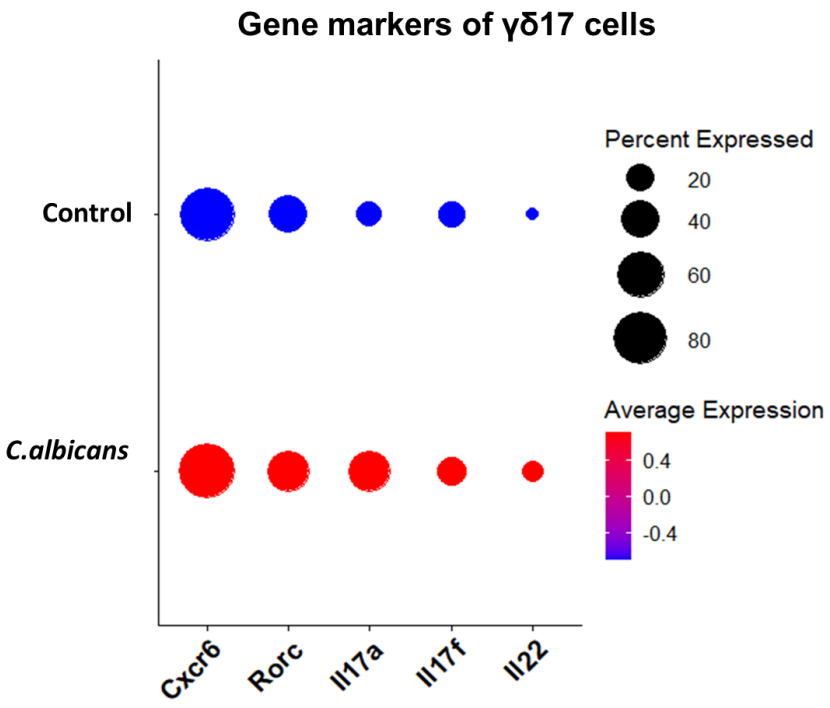

B

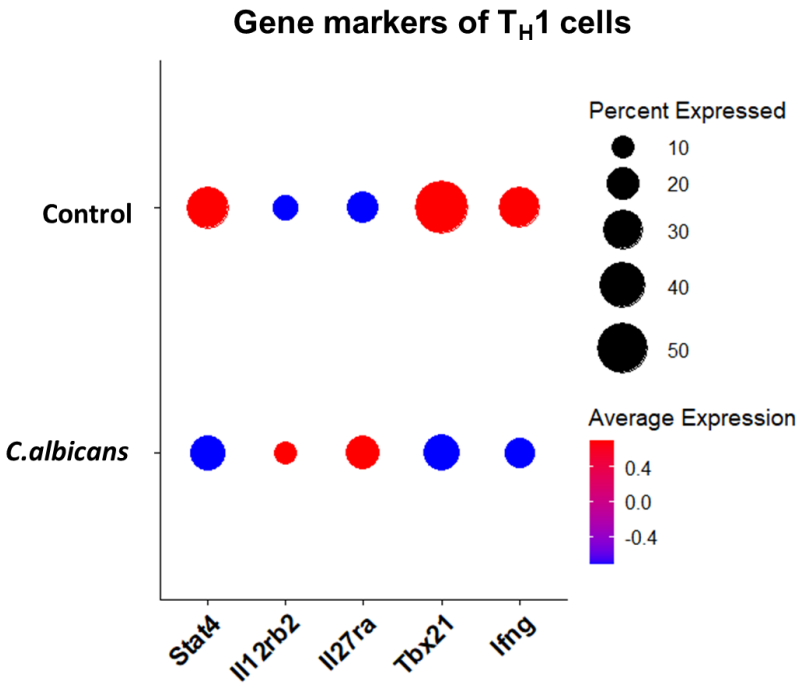

C

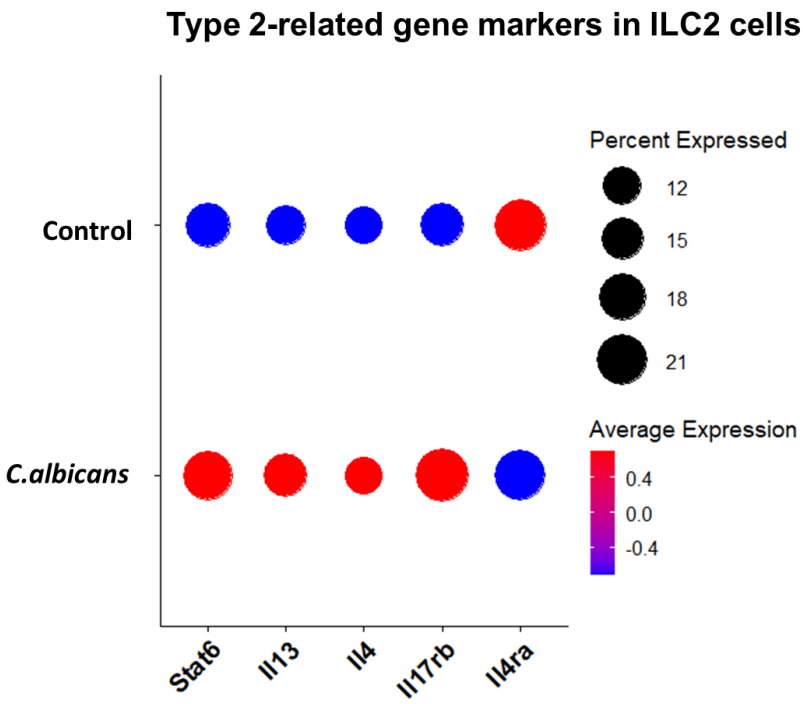

D

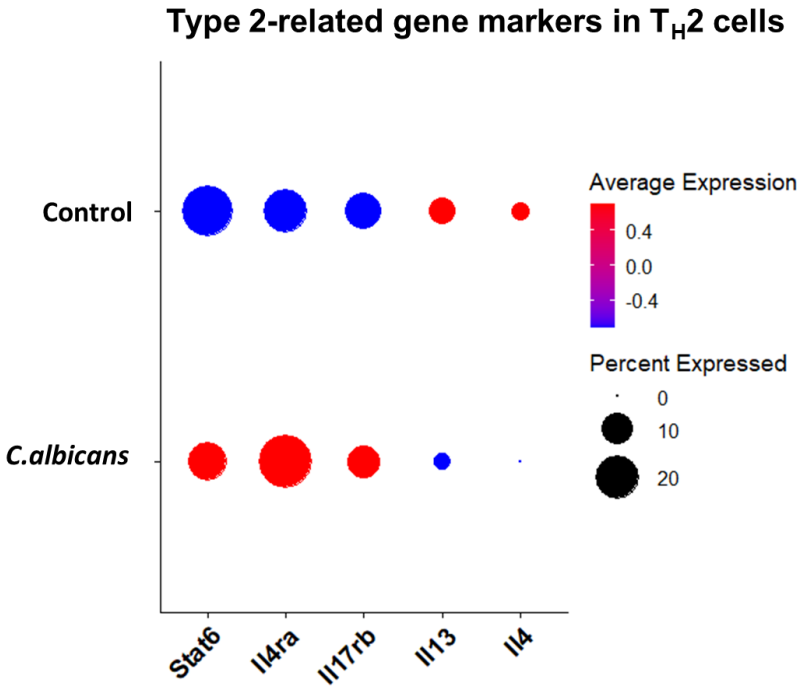

Figure 9. Assessment of Type 2 immune cells involvement in mediating itch in *C.albicans*-induced itch mouse model. (A) Dot Plot of Type 17-related gene markers' expression showing their upregulation in *C.albicans*-treated mice compared to the control group. (B) Dot Plot of T_H1-related gene markers' expression showing no difference between *C.albicans*-treated and control groups. (C) Dot Plots of Type 2 immune cell-related gene markers in ILC2 and (D) T_H2 clusters. Consistent increase in expression of genes was observed in ILC2 subset in *C.albicans*-treated group compared to control mice. Additionally, T_H2 cells showed tendency to increased expression of their gene markers in *C.albicans*-treated mice. The dot size shows the percentage of (C) γδ17, (D) T_H1, (E) ILC2 and (F) T_H2 immune cells that express corresponding genes, and the color represents the average expression of normalized transcript counts in of (C) γδ17, (D) T_H1, (E) ILC2 and (F) T_H2 immune cells.

3.4. Measurement of *C.albicans*-specific IgE in sera by enzyme linked immunosorbent assay (ELISA)

Based on our transcriptomic analysis results, in order to check the possible involvement of T_H2 cells in *C.albicans*-induced itch signal transduction, we further performed ELISA to measure *C.albicans*-specific IgE in *C.albicans*-treated mice. For this, we checked IgE level in serum collected on day 10 following our established protocol. According to our data, IgE was increased in *C.albicans* group compared to the control mice (Figure 10). Thus, these results support our hypothesis that *C.albicans* can trigger itch via activation of Type 2 immune response.

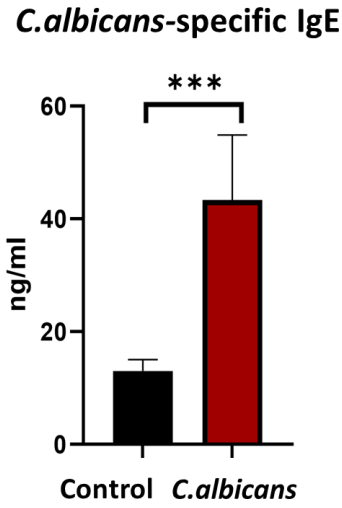

Figure 10. Measurement of *C.albicans*-specific IgE serum level in mouse *C.albicans*-induced itch model. *C.albicans*-specific IgE level in serum was elevated in *C.albicans* mice compared to the control group. Nonparametric Wilcoxon rank sum test was performed in Seurat to analyze statistical significance for (B). ***p <0.001.

4. DISCUSSION

"Itch-scratch cycle" is a debilitating feature that underlies a range of inflammatory dermatoses. Recently, skin has been recognized as a complex barrier organ capable of synchronizing neuronal and immune cells' activation in response to microbiota. *C.albicans* is a commensal fungus asymptomatically colonizing human barrier tissues including skin. It has been known that any skin barrier dysfunction leads to increased fungal load and subsequent activation of T_H17 cells in response to skin infection. However, the precise mechanisms of pruritis induced by *C. albicans* are yet to be discovered. Therefore, here we established a murine model of *C. albicans* skin infection to assess mechanisms underlying itch sensation. First, we evaluated itching behavior under application of *C.albicans* in different concentrations and confirmed most prominent scratching pattern when applied in 10^5 CFU/mL. Up to date, distinguishing itch-mediating and pain-mediating sensory neurons is a subject of debate, so we used oral model of *C.albicans* infection to confirm concentrations that triggers pain sensation. This resulted in increased wiping behavior when *C.albicans* was applied in concentration of 10^7 CFU/mL (Figure S1). Thus, our data showed dose-dependent behavior pattern when lower concentrations induced itch while higher doses mediated pain. To determine optimal time point for *C.albicans* epicutaneous application ,we conducted behavioral experiment in a time series manner and observed most stable pattern on day 10. Decrease in scratching behavior on day 12 can be possibly explained by hair follicle cycle that prevents efficient contact between *C.albicans* and epidermis. Taken together, we used concentration of 10^5 CFU/mL for daily epicutaneous application through 10 days as the most optimal scheme for establishment of *C.albicans*-induced itch mouse model.

We further assessed morphological and electrophysiological changes of sensory neurons triggered by *C.albicans*-induced itch. By conducting in vivo Imaging, we observed thickening and increased density of skin nerve fibers in *C.albicans*-treated mice along with enhanced neuronal responsiveness for stimulation assessed by VSDi. These observations suggest peripheral sensitization of cutaneous sensory neurons in response to repetitive *C.albicans* stimulation where neuronal cells become more reactive by changing membrane potential and lowering threshold for activation. Moreover, structural changes may reflect dynamic plasticity of sensory neurons where itch-specific neuronal subsets (NP) are upregulated as a form of functional adaptation to itch sensation.

We next conducted scRNA sequence analysis to explore neuro-immune crosstalk in *C.albicans*-induced itch mouse model in more depth. Consistent with previous studies, we were able to define 13 distinct clusters of neuronal cells. Usoskin et al. made the first attempt to analyze around 800 DRG neuronal cells and, in particular, using PCA analysis categorized C-type unmyelinated neuronal cells into non-peptidergic (NP) categories: NP1, NP2 and NP3, annotating them as itch-mediating neurons. Thus, NP1 subtype is presented by MrgprD^{+} polymodal sensory neurons that can transduce non-histaminergic itch sensation, including cholestatic itch; NP2 neurons are classified as MrgprA3^{+} neurons mediating itch induced by histamine and specifically by MrgprA3 agonists (chloroquine); and NP3 neuronal subset expressing *Sst* and IL31R that is engaged in transduction of inflammatory itch. In particular, LK Oetjen et al showed that Type 2 cytokines are able to sensitize neurons and amplify scratching behavior to other pruritogens applied in low doses. In this study, we found increased expression of Type 2 cytokine receptors in distinct NP subset with IL-4R being upregulated in NP1 and IL-13R upregulated in NP2 subsets. Moreover, we observed increased expression of histamine receptors in NP2 and NP3 neuronal subtypes. We further assessed Type 2 immune cell-related gene expression in T_H2 and ILC2 subsets. Our results show the increased expression of IL-4 and IL-13 cytokines along with transcriptional factor STAT6 and surface receptor IL-25R and IL13R in ILC2 subset from *C.albicans*-treated mice. Additionally, increased expression of STAT6, IL-4R, and IL-25R was confirmed in T_H2 cells. Thus, we speculate that *C.albicans* induces itch via enhanced Type 2 immune response that involves ILC2/T_H2 cells.

Given that Type 2 immune response was upregulated in *C.albicans*-induced itch mouse model, we evaluated *C.albicans*-specific IgE level in *C.albicans*-treated mouse group and their control littermates. According to our results, increased *C.albicans*-specific IgE serum level was observed in *C.albicans*-treated group, suggesting possible activation of B cells with subsequent production of specific IgEs as a response to *C.albicans*-induced itch and activation of Type 2 immune response in this model.

5. CONCLUSION

In summary, here we established *C.albicans*-induced itch mouse model in order to investigate driving mechanisms of itch sensation triggered by neuro-immune interaction under *C.albicans* application. *C.albicans*-induced itch leads to cutaneous sensory neurons remodeling and upregulation of Type 2 cytokine receptors in itch-specific NP neuronal subtypes. Moreover, upregulation of Type 2 related genes in ILC2/T_H2 population with increase production of *C.albicans*-specific IgE reflects enhanced Type 2 immune response unveiling one of the itch-mediating mechanisms in *C.albicans*-induced itch mouse model.

References

1. Wang F., Kim BS. Itch: A Paradigm of Neuroimmune Crosstalk. *Immunity*. 2020. 52(5):753-766.
2. Feuillet V, Ugolini S, Reynders A. Differential regulation of cutaneous immunity by sensory neuron subsets. *Trends Neurosci.* 2023. 46(8):640-653.
3. Agelopoulos K, Pereira MP, Wiegmann H, Ständer S. Cutaneous neuroimmune crosstalk in pruritus. *Trends Mol Med*. 2022. (6):452-462.
4. Oetjen LK, Mack MR, Feng J, Whelan TM, Niu H, Guo CJ, et al. Sensory Neurons Co-opt Classical Immune Signaling Pathways to Mediate Chronic Itch. *Cell*. 2017. 171(1):217-228.e13.
5. Tominaga M, Takamori K. Itch and nerve fibers with special reference to atopic dermatitis: therapeutic implications. *J Dermatol*. 2014. 41(3):205-12.
6. Riol-Blanco L, Ordovas-Montanes J, Perro M, Naval E, Thiriot A, Alvarez D, et al. Nociceptive sensory neurons drive interleukin-23-mediated psoriasiform skin inflammation. *Nature*. 2014. 510(7503):157-61.
7. Zhang X, Cao J, Zhao S, Yang X, Dong J, Tan Y, et al. Nociceptive Sensory Fibers Drive Interleukin-23 Production in a Murine Model of Psoriasis via Calcitonin Gene-Related Peptide. *Front Immunol*. 2021. 12:743675.
8. Deng L, Costa F, Blake KJ, Choi S, Chandrabalan A, Yousuf MS, et al. S. aureus drives itch and scratch-induced skin damage through a V8 protease-PAR1 axis. *Cell*. 2023. 186(24):5375-5393.e25.
9. Enamorado M, Kulalert W, Han SJ, Rao I, Delaleu J, Link VM, et al. Immunity to the microbiota promotes sensory neuron regeneration. *Cell*. 2023. 186(3):607-620.e17.
10. Filtjens J, Roger A, Quatrini L, Wieduwild E, Gouilly J, Hoeffel G, et al. Nociceptive sensory neurons promote CD8 T cell responses to HSV-1 infection. *Nat Commun*. 2021. 12(1):2936.
11. Verzosa AL, McGeever LA, Bhark SJ, Delgado T, Salazar N, Sanchez EL. Herpes Simplex Virus 1 Infection of Neuronal and Non-Neuronal Cells Elicits Specific Innate Immune Responses and Immune Evasion Mechanisms. *Front Immunol*. 2021. 12:644664.
12. Kashem SW, Riedl MS, Yao C, Honda CN, Vulchanova L, Kaplan DH. Nociceptive Sensory Fibers Drive Interleukin-23 Production from CD301b+ Dermal Dendritic Cells and Drive Protective Cutaneous Immunity. *Immunity*. 2015. 43(3):515-26.
13. Yosipovitch G, Kim B, Luger T, Lerner E, Metz M, Adiri R, et al. Similarities and differences in peripheral itch and pain pathways in atopic dermatitis. *J Allergy Clin Immunol.* 2024. 153(4):904-912.
14. Suehiro M, Numata T, Saito R, Yanagida N, Ishikawa C, Uchida K, et al. Oncostatin M suppresses IL31RA expression in dorsal root ganglia and

interleukin-31-induced itching. *Front Immunol*. 2023. 14:1251031.
15. Abreu M, Miranda M, Castro M, Fernandes I, Cabral R, Santos AH, et al. IL-31 and IL-8 in Cutaneous T-Cell Lymphoma: Looking for Their Role in Itch. *Adv Hematol*. 2021. 2021:5582581.
16. Netea MG, Joosten LA, van der Meer JW, Kullberg BJ, van de Veerdonk FL. Immune defence against Candida fungal infections. Nat Rev Immunol. 2015. (10):630-42.
17. Park CO, Fu X, Jiang X, Pan Y, Teague JE, Collins N et al. Staged development of long-lived T-cell receptor αβ TH17 resident memory T-cell population to *Candida albicans* after skin infection. *J Allergy Clin Immunol*. 2018. 142(2):647-662
18. Sherman F. Getting started with yeast. *Methods Enzymol*. 1991. 194:3–21
19. Solis NV, Filler SG. Mouse model of oropharyngeal candidiasis. *Nat. Protoc*. 2012. 7:637–642.
20. LaMotte RH, Shimada SG, Sikand P. Mouse models of acute, chemical itch and pain in humans. *Exp Dermatol*. 2011. 20(10):778–782.
21. Pinho-Ribeiro FA, Baddal B, Haarsma R, O'Seaghdha M, Yang NJ, Blake KJ et al. Blocking Neuronal Signaling to Immune Cells Treats Streptococcal Invasive Infection. *Cell*. 2018. 173(5):1083-1097.e22.
22. Li J.L., Goh C.C., Keeble J.L., Qin J.S., Roediger B., Jain R. et al. Intravital multiphoton imaging of immune responses in the mouse ear skin. *Nat Protocols*. 2012. 7, 221-234
23. Kwon M, Jung IY, Cha M, Lee BH. Inhibition of the Nav1.7 Channel in the Trigeminal Ganglion Relieves Pulpitis Inflammatory Pain. Front Pharmacol. 2021. 8:12:759730
24. Mecklenburg J, Shein SA, Malmir M, Hovhannisyan AH, Weldon K, Zou Y, et al. Transcriptional profiles of non-neuronal and immune cells in mouse trigeminal ganglia. *Front Pain Res (Lausanne)*. 2023 Oct 31; 4:1274811
25. Chen R, McVey DG, Shen D, Huang X, Ye S. Phenotypic Switching of Vascular Smooth Muscle Cells in Atherosclerosis. *J Am Heart Assoc*. 2023 Oct 17;12(20): e031121
26. Bjørklund G, Svanberg E, Dadar M, Card DJ, Chirumbolo S, Harrington DJ et al. The Role of Matrix Gla Protein (MGP) in Vascular Calcification. *Curr Med Chem*. 2020. 27(10):1647-1660
27. Hashimoto Y, Greene C, Munnich A, Campbell M. The CLDN5 gene at the blood-brain barrier in health and disease. Fluids and Barriers of the CNS. 2023. 20, 22 (2023).
28. Chu Y, Jia, S., Xu, K., Liu, Q., Mai, L., Liu, J., et al. Single-cell transcriptomic profile of satellite glial cells in trigeminal ganglion. *Front Mol Neurosci*. 2023. 16, 1117065.
29. Jessen KR, Mirsky R. Schwann Cell Precursors; Multipotent Glial Cells in Embryonic Nerves. *Front Mol Neurosci*. 2019. 12:69

30. Zou M, Li S, Klein WH, Xiang M. Brn3a/Pou4f1 regulates dorsal root ganglion sensory neuron specification and axonal projection into the spinal cord. *Dev Biol*. 2012 Apr 15;364(2):114-27
31. Qi L, Iskols M, Shi D, Reddy P, Walker C, Lezgiyeva K, et al. A mouse DRG genetic toolkit reveals morphological and physiological diversity of somatosensory neuron subtypes. *Cell*. 2024. 187(6):1508-1526.e16
32. Casanovas S, Schlichtholz L, Mühlbauer S, Dewi S, Schüle M, Strand D, et al. Rbfox1 Is Expressed in the Mouse Brain in the Form of Multiple Transcript Variants and Contains Functional E Boxes in Its Alternative Promoters. *Front Mol Neurosci*. 2020. 13:66
33. Jacko M, Weyn-Vanhentenryck SM, Smerdon JW, Yan R, Feng H, Williams DJ, et al. Rbfox Splicing Factors Promote Neuronal Maturation and Axon Initial Segment Assembly. *Neuron*. 2018 Feb 21;97(4):853-868.e6.
34. Renthal W, Tochitsky I, Yang L, Cheng YC, Li E, Kawaguchi R, et al. Transcriptional Reprogramming of Distinct Peripheral Sensory Neuron Subtypes after Axonal Injury. *Neuron*. 2020. 108(1):128-144.e9
35. Usoskin D, Furlan A, Islam S, Abdo H, Lönnerberg P, Lou D, et al. Unbiased classification of sensory neuron types by large-scale single-cell RNA sequencing. Nat Neurosci. 2015. (1):145-53.
36. Wang K, Cai B, Song Y, Chen Y, Zhang X. Somatosensory neuron types and their neural networks as revealed via single-cell transcriptomics. *Trends Neurosci*. 2023 Aug;46(8):654-666.
37. Lay M, Dong X. Neural Mechanisms of Itch. *Annu Rev Neurosci*. 2020. 43:187-205.
38. Guo CJ, Grabinski NS, Liu Q. Peripheral Mechanisms of Itch. *J Invest Dermatol*. 2022. 142(1):31-41.
39. Facheris P, Jeffery J, Del Duca E, Guttman-Yassky E. The translational revolution in atopic dermatitis: the paradigm shift from pathogenesis to treatment. *Cell Mol Immunol*. 2023. (5):448-474
40. Moniaga CS, Tominaga M, Takamori K. The Pathology of Type 2 Inflammation-Associated Itch in Atopic Dermatitis. *Diagnostics (Basel)*. 2021. 11(11):2090
41. Zhu K, Cai L, Cui C, de Los Toyos JR, Anastassiou D. Single-cell analysis reveals the pan-cancer invasiveness-associated transition of adipose-derived stromal cells into COL11A1-expressing cancer-associated fibroblasts. *PLoS Comput Biol*. 2021. 17(7): e1009228
42. Muhl L, Genové G, Leptidis S, Liu J, He L, Mocci G, et al. Single-cell analysis uncovers fibroblast heterogeneity and criteria for fibroblast and mural cell identification and discrimination. *Nat Commun*. 2020. 11(1):3953.
43. Ascensión AM, Fuertes-Álvarez S, Ibañez-Solé O, Izeta A, Araúzo-Bravo MJ. Human Dermal Fibroblast Subpopulations Are Conserved across Single-Cell RNA Sequencing Studies. *J Invest Dermatol*. 2021. 141(7):1735-1744.e35
44. Cheng JB, Sedgewick AJ, Finnegan AI, Harirchian P, Lee J, Kwon S, et al.

Transcriptional Programming of Normal and Inflamed Human Epidermis at Single-Cell Resolution. Cell Rep. 2018. 25(4):871-883

45. Leyva-Castillo JM, Sun L, Wu SY, Rockowitz S, Sliz P, Geha RS. Single-cell transcriptome profile of mouse skin undergoing antigen-driven allergic inflammation recapitulates findings in atopic dermatitis skin lesions. *J Allergy Clin Immunol*. 2022. 150(2):373-384
46. Rheinländer A, Schraven B, Bommhardt U. CD45 in human physiology and clinical medicine. *Immunol Lett*. 2018. 196:22-32.
47. Schupp JC, Adams TS, Cosme C Jr, Raredon MSB, Yuan Y, Omote N, et al. Integrated Single-Cell Atlas of Endothelial Cells of the Human Lung. *Circulation*. 2021.144(4):286-302.
48. Guo, D., Li, X., Wang, J.et al. Single-cell RNA-seq reveals keratinocyte and fibroblast heterogeneity and their crosstalk via epithelial-mesenchymal transition in psoriasis. *Cell Death Dis.* 2024. 15, 207
49. Medic S, Ziman M. PAX3 expression in normal skin melanocytes and melanocytic lesions (naevi and melanomas). *PLoS One*. 2010. 5(4): e9977
50. Harris ML, Baxter LL, Loftus SK, Pavan WJ. Sox proteins in melanocyte development and melanoma. *Pigment Cell Melanoma Res*. 2010. (4):496-513.
51. Hoyle DJ, Rodriguez-Fernandez IA, Dell'angelica EC. Functional interactions between OCA2 and the protein complexes BLOC-1, BLOC-2, and AP-3 inferred from epistatic analyses of mouse coat pigmentation. *Pigment Cell Melanoma Res*. 2011. 24(2):275-81.
52. Dick SA, Wong A, Hamidzada H, Nejat S, Nechanitzky R, Vohra S, et al. Three tissue resident macrophage subsets coexist across organs with conserved origins and life cycles. *Sci Immunol.* 2022.7(67): eabf7777.
53. Waddell LA, Lefevre L, Bush SJ, Raper A, Young R, Lisowski ZM, et al. ADGRE1 (EMR1, F4/80) Is a Rapidly-Evolving Gene Expressed in Mammalian Monocyte-Macrophages. *Front Immunol*. 2018. 9:2246
54. Zhang S, Audiger C, Chopin M, Nutt SL. Transcriptional regulation of dendritic cell development and function. *Front Immunol.* 2023. 14:1182553
55. Liu X, Zhu R, Luo Y, Wang S, Zhao Y, Qiu Z, et al. Distinct human Langerhans cell subsets orchestrate reciprocal functions and require different developmental regulation. *Immunity*. 2021. 54(10):2305-2320.e11
56. Bosteels C, Neyt K, Vanheerswynghels M, van Helden MJ, Sichien D, Debeuf N et al. Inflammatory Type 2 cDCs Acquire Features of cDC1s and Macrophages to Orchestrate Immunity to Respiratory Virus Infection. *Immunity*. 2020. 52(6):1039-1056.e9.
57. Abbas AK, Lichtman AH, Pillai S. Differentiation and Functions of CD4+ Effector T Cells. In: Cellular and Molecular Immunology. 10th edition. Philadelphia: *Elsevier*; 2021. P.460-99.
58. Tauber M, Basso L, Martin J, Bostan L, Pinto MM, Thierry GR, et al. Landscape of mast cell populations across organs in mice and humans. *J Exp Med.* 2023.

220(10): e20230570.

59. Leyva-Castillo JM, Sun L, Wu SY, Rockowitz S, Sliz P, Geha RS. Single-cell transcriptome profile of mouse skin undergoing antigen-driven allergic inflammation recapitulates findings in atopic dermatitis skin lesions. *J Allergy Clin Immunol*. 2022 Aug;150(2):373-384.
60. Ran R, Trapecar M, Brubaker DK. Systematic Analysis of Human Colorectal Cancer scRNA-seq Revealed Limited Pro-tumoral IL-17 Production Potential in Gamma Delta T Cells. bioRxiv. 2024:07.18.604156.
61. Kagami S, Rizzo HL, Kurtz SE, Miller LS, Blauvelt A. IL-23 and IL-17A, but not IL-12 and IL-22, are required for optimal skin host defense against Candida albicans. *J Immunol*. 2010 Nov 1;185(9):5453-62.
62. Conti HR, Peterson AC, Brane L, Huppler AR, Hernández-Santos N, Whibley N, et al. Oral-resident natural Th17 cells and γδ T cells control opportunistic Candida albicans infections. *J Exp Med.* 2014 Sep 22;211(10):2075-84.
63. Kobayashi T, Moro K. Tissue-Specific Diversity of Group 2 Innate Lymphoid Cells in the Skin. Front Immunol. 2022. 13:885642.

Appendices 1.

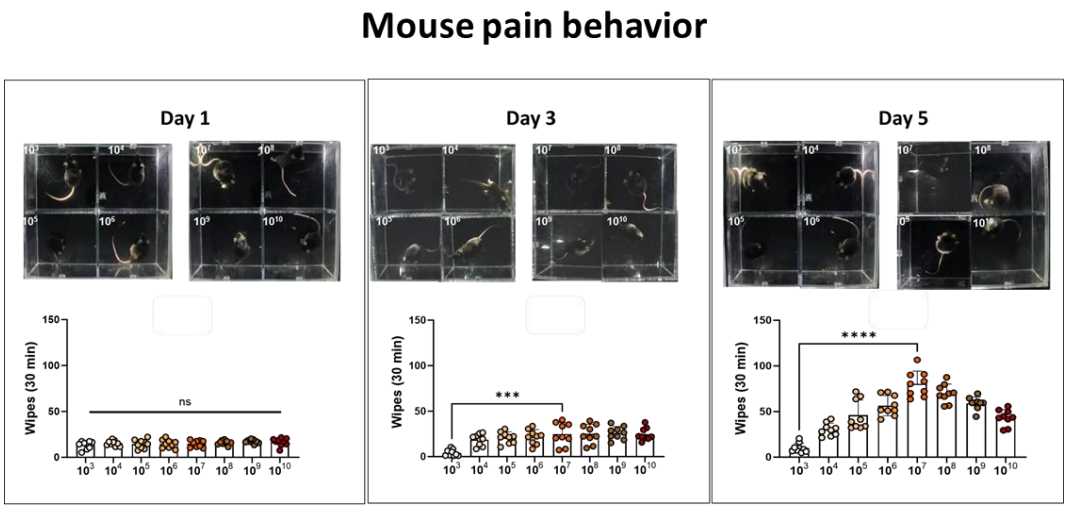

Figure S1. Assessment of mouse pain behavioral phenotype. Wiping behavior towards oral area of WT mice treated by various concentrations of *C.albicans* starting from low 10^3 to high 10^{10} CFU/mL (50 μl) via placing cotton swab sublingually, n ≥ 8 mice per group. Nonparametric Mann-Whitney U tests was performed to analyze statistical significance for (A) -(C). ***p < 0.001; ****p < 0.0001; ns, not significant.

Abstract in Korean

Candida albicans 유발 가려움증 마우스 모델에서 신경-면역 상호작용 규명을 위한 단일세포 전사체 분석

"가려움-긁음 사이클(Itch-scratch cycle)"은 다양한 염증성 피부질환에서 관찰되는 대표적인 만성 증상 중 하나로 환자의 삶의 질을 저하시킬 수 있습니다. 최근 피부는 미생물군에 반응하여 신경세포 및 면역세포의 활성을 동기화할 수 있는 복합적인 장벽 기관으로 인식되고 있습니다.

Candida albicans(칸디다 알비칸스)는 피부를 포함한 인체 장벽 조직에 무증상으로 공생하는 진균이며, 피부 장벽 기능이 손상될 경우 진균 부하가 증가하고 이에 따라 T_H17 세포의 활성화가 유도되는 것으로 알려져 있습니다. 하지만 *C. albicans* 피부 감염에 의해 유도되는 가려움증(pruritis)의 정확한 유발 기전은 아직 명확히 밝혀지지 않았습니다.

이에 본 연구에서는 *C. albicans* 피부 감염 마우스 모델을 수립하고, 감염에 따른 가려움 행동 표현형을 분석하고자 하였습니다. 일반적으로 가려움 감각은 제2형 면역반응과 밀접한 관련이 있는 것으로 알려져 있으므로, 본 연구에서는 *C. albicans*에 의해 유도된 가려움증에서의 제2형 면역 반응의 관여 여부와 작용 기전을 규명하고자 하였습니다. 이를 위해 마우스 피부 및 후근신경절 (Dorsal Root Ganglion, DRG)에 대해 단일세포 RNA 시퀀싱 분석을 수행하고 세포 간 상호작용을 분석하였습니다.

이와 같이 본 연구는 단일세포 전사체 분석을 통해 *C.albicans* 에 의해 유도되는 가려움 감각의 기전을 규명하고자 하는 초기 연구로서 기여하고자 합니다.

핵심되는 말: 칸디다 알비칸스, 가려움증, 신경-면역 상호작용, DRG, 제2형 면역반응